KeAi

CHINESE ROOTS
GLOBAL IMPACT

Contents lists available at ScienceDirect

#### Petroleum Science

journal homepage: www.keaipublishing.com/en/journals/petroleum-science



#### Original Paper

# Utilization mechanism of foam flooding and distribution situation of residual oil in fractured-vuggy carbonate reservoirs



Yu-Chen Wen <sup>a, b</sup>, Ji-Rui Hou <sup>a, b</sup>, Xiao-Li Xiao <sup>a, b</sup>, Chang-Ming Li <sup>a, b</sup>, Ming Qu <sup>a, b, \*</sup>, Ya-Jie Zhao <sup>a, b</sup>, Wei-Xin Zhong <sup>a, b</sup>, Tuo Liang <sup>a, b</sup>, Wei-Peng Wu <sup>a, b</sup>

#### ARTICLE INFO

# Article history: Received 6 July 2022 Received in revised form 11 November 2022 Accepted 23 November 2022 Available online 5 December 2022

Edited by Yan-Hua Sun

Keywords: Fractured-vuggy reservoirs Foam flooding Physical model Residual oil Enhanced oil recovery (EOR)

#### ABSTRACT

The development of fractured-vuggy carbonate reservoirs is extremely difficult because of the complex fractured-vuggy structure and strong heterogeneity. Foam flooding is a potential enhanced oil recovery (EOR) technology in fractured-vuggy carbonate reservoirs. Based on the similarity criterion, three types of 2D visual physical models of the fractured-vuggy structure were made by laser ablation technique, and a 3D visual physical model of the fractured-vuggy reservoir was made by 3D printing technology. Then the physical analog experiments of foam flooding were carried out in these models. The experimental results show that foam can effectively improve the mobility ratio, control the flow velocity of the fluid in different directions, and sweep complex fracture networks. The effect of foam flooding in fractures can be improved by increasing foam strength and enhancing foam stability. The effect of foam flooding in vugs can be improved by reducing the density of the foam and the interfacial tension between foam and oil. Three types of microscopic residual oil and three types of macroscopic residual oil can be displaced by foam flooding. This study verifies the EOR of foam flooding in fractured-vuggy reservoir and provides theoretical support for the application of foam flooding in fractured-vuggy reservoirs.

© 2023 The Authors. Publishing services by Elsevier B.V. on behalf of KeAi Communications Co. Ltd. This is an open access article under the CC BY-NC-ND license (http://creativecommons.org/licenses/by-nc-nd/4.0/).

#### 1. Introduction

As an important part of the world's oil and gas resources, carbonate reservoirs are widely distributed all over the world, and their oil and gas reserves account for more than half of the world's reserves (Dai et al., 2018; Lu et al., 2022). Ordovician fractured-vuggy carbonate reservoir is the largest carbonate reservoir in China in terms of reservoirs (Hou et al., 2016). The fractured-vuggy in the fractured-vuggy carbonate reservoir is mainly composed of three types, including underground river, vugs, and fractured-vuggy (Li and Fan, 2011). Therefore, the fractured-vuggy carbonate reservoir has a diverse morphology in structure, an obvious difference in size, and a strong heterogeneity in formation (Qu et al., 2020a). The permeability of the carbonate matrix is extremely low, which ranges from 0.1 to 1 mD (Hou et al., 2018). Oil and gas are mainly stored in large fractures and large vugs, in which

the flow of fluids mainly depends on fractures (Chen et al., 2005). The above characteristics lead to a difficult development and a low oil recovery ratio in carbonate reservoirs. In recent years, China has made significant progress in the development of fractured-vuggy carbonate reservoirs, with the increasingly mature development methods of fractured-vuggy carbonate reservoirs (Lu et al., 2022).

Generally, depletion development is adopted in the initial stage of production of fractured-vuggy carbonate reservoirs. During the natural energy development phase, the initial production of the Tahe Oilfield was high, but the formation energy decreased rapidly. The final oil recovery ratio in the natural energy development phase was 8%–14% (Wang et al., 2020). Then water drive and gas drive were carried out in the Tahe Oilfield (Rong et al., 2013; Song et al., 2016; Wang et al., 2020; Yuan et al., 2015). However, due to the complex reservoir characteristics of the fractured-vuggy reservoir, water channeling and gas channeling are easy to occur during the development process, resulting in the unsatisfactory recovery of the fractured vuggy reservoir (Liang et al., 2021; Qu et al., 2018; Rong et al., 2008; Wang et al., 2019).

Foam flooding in fractured-vuggy carbonate reservoirs has been

<sup>&</sup>lt;sup>a</sup> Research Institute of Unconventional Petroleum Science and Technology, China University of Petroleum (Beijing), Beijing, 102249, China

<sup>&</sup>lt;sup>b</sup> Key Laboratory of Petroleum Engineering, China University of Petroleum (Beijing), Beijing, 102249, China

<sup>\*</sup> Corresponding author. Research Institute of Unconventional Petroleum Science and Technology, China University of Petroleum (Beijing), Beijing, 102249, China. *E-mail address:* m.qu@foxmail.com (M. Qu).

studied in recent years, and foam flooding has been proven to be beneficial to the development of fractured-vuggy carbonate reservoirs (Yang and Hou, 2020). Research showed that foam can control gas fluidity and effectively inhibit gas channeling (Talebian et al., 2014). Foam can significantly improve oil recovery ratio by expanding sweep volume and improving displacement efficiency (Telmadarreie and Trivedi, 2017; Wen et al., 2019). Yang et al. (2019) synthesized a gel system of foam, and verified the plugging properties and the improved oil recovery ratio of the foam. Su et al. (2017) designed and manufactured a visual physical model of fractured-vuggy carbonate reservoirs, and carried out physical simulation experiments to verify the EOR of foam. Wang et al. (2015) carried out foam flow experiments and found that the foam resistance factor gradually diminished as the liquid flow rate increased with a constant gas flow rate.

At present, the research on residual oil in fractured-vuggy reservoirs is mainly carried out in three aspects, including physical experiments, numerical simulations, and field summaries. Chen et al. (2014) proposed a Robin-Robin domain decomposition method for the coupled system with the generalized Navier interface boundary condition at the interface between the free flow and the porous media regions. However, for the complex fracturedvuggy structure, the calculation method is difficult to operate and does not have much practicability. Liu et al. (2020) proposed an efficient hybrid model for the characterization and simulation of 3D complex fractured-vuggy reservoirs, and simulated the production dynamics of the actual reservoir. However, for the complexity of the flow mechanism and numerical solution, applying numerical simulation to analyze the residual oil distribution is still a difficult problem. Field summary usually analyzes the residual oil by fine description and production performance, but the field summary lacks a refined description of residual oil distribution in fracturedvuggy reservoirs (Lu et al., 2022). The physical experiment is an important technology to analyze the distribution of residual oil. Li et al. (2009) classified the residual oil into continuous and dispersed types through the photoetching microscopic plane model. By establishing the quantitative model and stochastic model of fractured-vuggy reservoirs, Wang et al. (2012) summarized the residual oil as occlusion oil, attic oil, corner oil, blind cavity oil, and oil film. Xie (2019) studied the influencing factors of the residual oil, and analyzed the formation mechanism of the residual oil from the perspective of mechanics. Hou et al. (2018) developed a 2D microscopic visual physical model to analyze the distribution law of residual oil intuitively.

However, the research on residual oil distribution after foam flooding in fractured-vuggy carbonate reservoirs is rare, and there is no clear understanding of the distribution of residual oil after foam flooding in fractured-vuggy carbonate reservoirs. With the constantly advancement of the pilot test of EOR in Tahe Oilfield, it is necessary to study the sweep mechanisms and distribution of residual oil after foam flooding in fractured-vuggy carbonate reservoirs (Lu et al., 2022).

In this paper, the model parameters and experimental parameters of physical simulation are designed according to the similarity criteria. Three kinds of 2D visual physical models of fractured-vuggy structure and a 3D visual physical model of fractured-vuggy reservoir are made. Experimental studies of water flooding, nitrogen gas flooding, and foam flooding in different fractured-vuggy models are carried out. According to the experimental results, the characteristics and mechanism of foam flooding in fractured-vuggy reservoirs are studied. The flow laws in different directions in fractured-vuggy structure are clarified, and the distribution characteristics of residual oil after different flooding methods are analyzed. The sweep mechanisms of foam on residual oil in the fractured-vuggy structure are revealed, and the oil

recovery ratio of foam flooding in the fractured-vuggy reservoir is verified. This paper provides theoretical support for sweeping the residual oil by foam flooding in fractured-vuggy carbonate reservoirs.

#### 2. Physical model design and fabrication

In this study, a visual physical simulation method is used to study the sweep mechanism of foam flooding and the distribution of residual oil in fractured-vuggy carbonate reservoirs. The parameters of physical models were designed based on similarity criteria, including 2D visual physical model of fractured-vuggy structure and 3D visual physical model of fractured-vuggy reservoir. Due to the extremely low matrix permeability of fracturedvuggy carbonate reservoirs, the fluid in the matrix basically has no flow ability. The fluid migration conforms to Newton's law and thermodynamic laws in the reservoirs. As long as the influencing factors in the fluid motion equation are similar, the flow of fluid is similar (as showed in Table 1). In this study, the fractures and karst caves characteristic parameters of the visual physical model were designed by geometric similarity. The physical properties and the injection parameters of fluid were designed by the kinematic similarity and dynamic similarity. The specific design method was introduced in detail in the previous research (Qu et al., 2020a). This design ensured the similarity of the fluid flow in the fracturedvuggy physical model and in the actual reservoir. The 2D visual physical model of fractured-vuggy structure was designed and manufactured based on the simplified typical fractured-vuggy structure of the actual reservoir in Tahe Oilfield. The 3D visual physical model of fractured-vuggy reservoir was designed and manufactured by scaling down the actual fractured-vuggy reservoir in the TK425CH well group of Tahe Oilfield.

#### 2.1. 2D visual physical model of fractured-vuggy structure

The 2D visual physical model of fractured-vuggy structure was designed to study the sweep mechanism and microscopic distribution of residual oil in fractured-vuggy structure after foam flooding. It can intuitively study the fluid distribution in various fractured-vuggy structures after foam flooding. Two conditions of the 2D visual physical model of fractured-vuggy structure were designed in this study including filled models and unfilled models.

The design drawings of models were designed according to the simplified typical fractured-vuggy structure. Then the fractured-vuggy structure was etched on the acrylic sheet (the surface wettability of the acrylic plate is oil-wet). After covering another acrylic sheet on the first acrylic sheet, they were bonded and sealed at high temperature. The outline dimension of 2D visual physical model of fractured-vuggy structure was  $10~{\rm cm}\times 10~{\rm cm}\times 2~{\rm cm}$ . The filler used in the model is lipophilic transparent acrylic beads with a diameter of 2 mm. Three 2D visual fractured-vuggy physical models were designed and manufactured in this study, including fractured model (Fig. 1), vuggy model (Fig. 2), and fractured-vuggy model (Fig. 3).

# 2.2. 3D visual physical model of fractured-vuggy carbonate reservoir

3D visual physical model of fractured-vuggy reservoir is used to study the macroscopic distribution of residual oil and the displacement effect after foam flooding in the fractured-vuggy carbonate reservoir. The macroscopic phenomenon of fluid flow in the model is more obvious than that in the 2D visual physical model.

This kind of model was made by 3D printing technology. The internal fractured-vuggy structure was designed according to the

**Table 1** Similarity criteria.

Similarity conditions	Similarity criteria	Physical significance	Similarity index
Geometric similarity	$\pi_1 = d/l$	Ratio of the cavity diameter to the reservoir controlled diameter	1
	$\pi_2 = B/l$	Ratio of the fracture aperture to the reservoir controlled diameter	1
Dynamic similarity	$F_{\rm G} = \Delta P/(\rho_{\rm o} g d)$	Ratio of the injected pressure to gravity	1.01-1.04
	$Re = \rho u l / \mu$	Ratio of the moving inertial force to the viscous force	1
Kinematic similarity	$F_O = Q/(r^2u)$	Ratio of the recovery volume to the injection volume	1.01-1.04
Characteristic similarity	$\Pi_3 = \xi$	Coordination number	1
	$\Pi_4 = \eta$	Filled degree	1

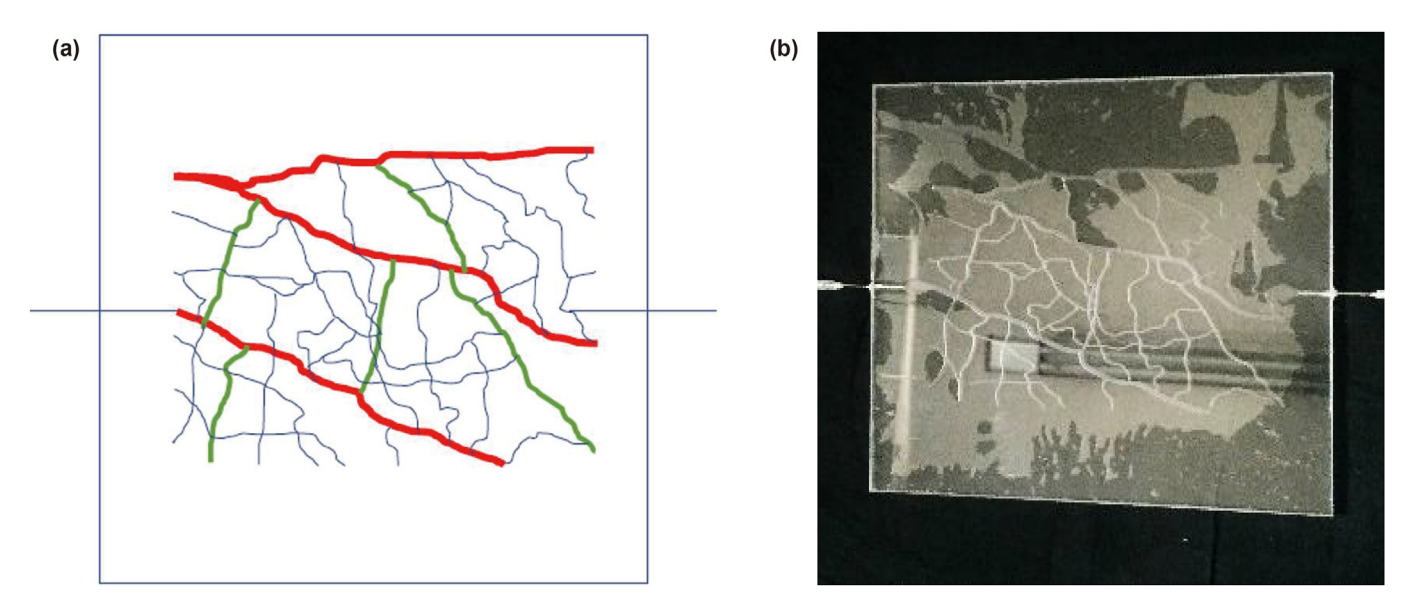


Fig. 1. Schematic of the 2D visual fractured model. (a) Design drawing; (b) Physical model. The width of the red fracture is 2 mm, the width of the green fracture is 1 mm, and the width of the blue fracture is 0.5 mm.

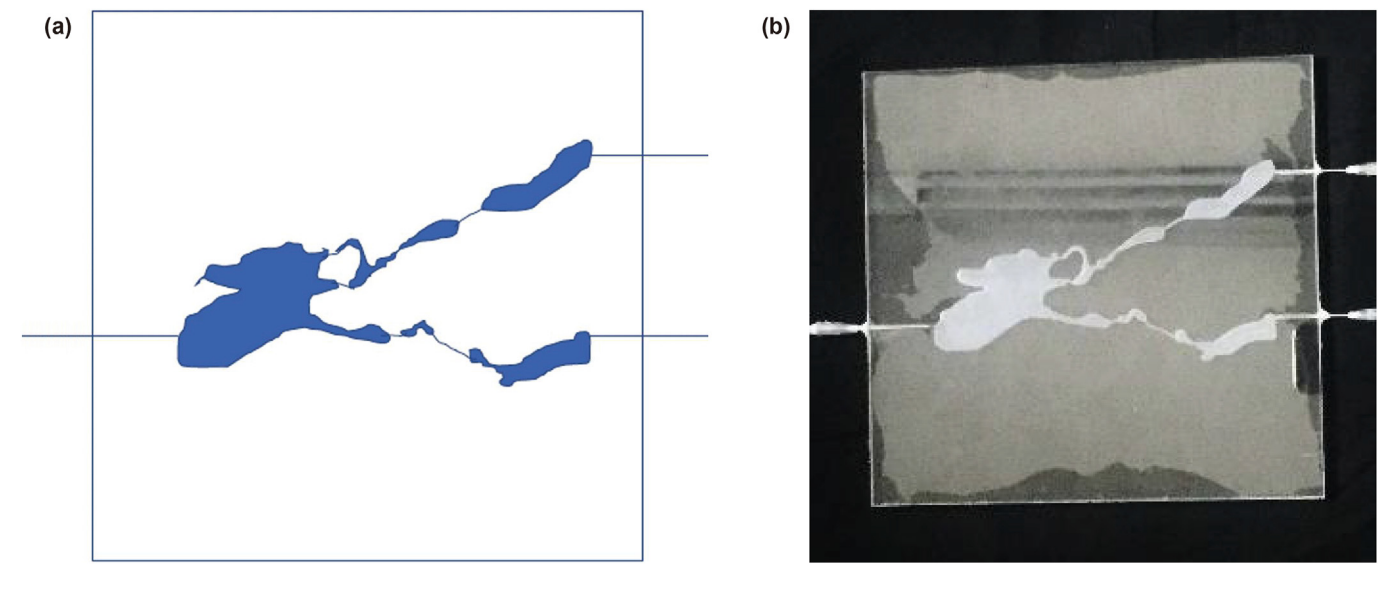
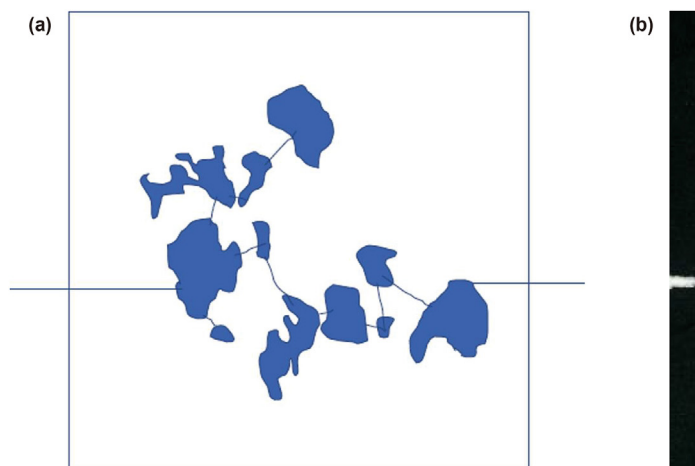


Fig. 2. Schematic of the 2D visual vuggy model. (a) Design drawing; (b) Physical model. The widest part of the vug is 45 mm, and the narrowest part of it is 1 mm.

3D geological data of TK425CH well group in the Tahe Oilfield. As shown in Figs. 4 and 5, nine cross sections of the formation of this well group were intercepted at equal distances. The obtained cross sections of the fractured-vuggy structure were imported into 3D simulation software. After optimizing the fractured-vuggy

structure of the cross sections, the 3D model design drawing was obtained. Then the 3D visual model was manufactured using the 3D printer. Fig. 6 shows the 3D visual physical model of the TK425CH well group, the outline dimension of this model was  $15~\text{cm} \times 8~\text{cm} \times 8~\text{cm}$ .



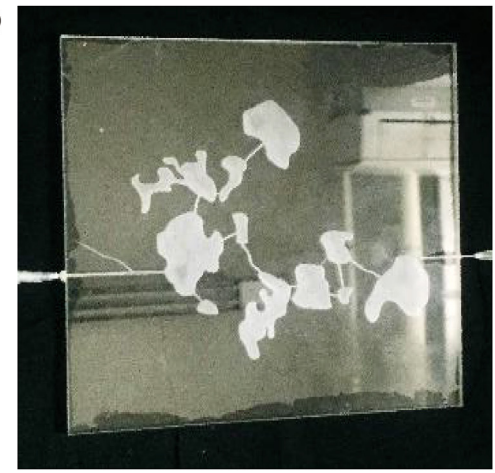


Fig. 3. Schematic of 2D visual fractured-vuggy model. (a) Design drawing; (b) Physical model. The width range of the vuggy is 5-40 mm and the width of the fracture is 1 mm.

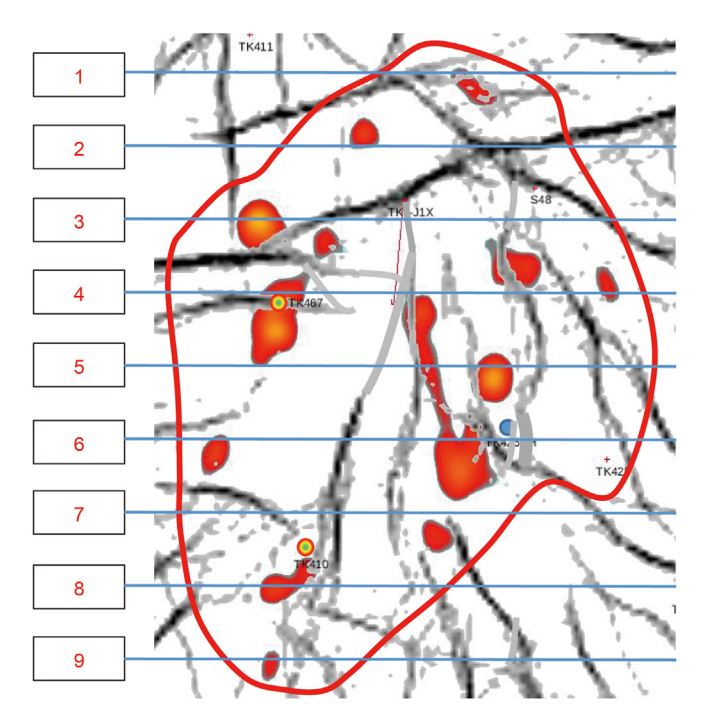


Fig. 4. The schematic drawing of cross section of TK425CH well group.

#### 3. Experimental materials and process

#### 3.1. Experimental materials

The fractured-vuggy reservoirs were characterized by high-temperature high-pressure and high-salinity in the Tahe Oilfield, which does not have a shear effect similar to porous media. Therefore, the high stability foam was used for foam flooding after foaming on the ground in the Tahe Oilfield. This kind of foam can migrate stably in the fractured-vuggy structure (Qu et al., 2020b). Chemical reagents for laboratory preparation of foam include: foaming agent (SS-163, 99 wt%, Qingdao Changxing Hi-tech Development Co., Ltd), sodium dodecyl sulfate (SDS, 99.7 wt%, Shanghai Macklin Biochemical Co., Ltd),  $\alpha$ -modified starch (80 wt%, Qingdao Changxing Hi-tech Development Co., Ltd), acrylamide (99.7 wt%, Shanghai Macklin Biochemical Co., Ltd), N,N'-methylenebisacrylamide (MBA, 99.7 wt%, Shanghai Macklin Biochemical

Co., Ltd), and potassium persulfate (99.7 wt%, Shanghai Macklin Biochemical Co., Ltd).

 $\alpha$ -modified starch (2 wt%), acrylamide (2 wt%), MBA (0.1 wt%), and potassium persulfate (0.01 wt%) were added to water and stirred until completely dissolved. A kind of weak gel was formed after this solution was placed in an oven at 100 °C for 1 h. The mixed liquid was formed with SS-163 (0.3 wt%), SDS (0.3 wt%), and the weak gel (after it was completely broken by the mixer). Finally, high stability foam is formed with nitrogen gas and mixed liquid in a gas—liquid ratio of 2:1.

Industrial nitrogen (purity 99.2%) was used in the experiment to produce foam. The experimental simulated oil was configured by liquid paraffin and kerosene in proportion. The viscosity of the simulated oil was 60 mPa s and the density of the simulated oil was 0.83 g/mL. The simulated oil was dyed red with Sudan Red for better observation. As shown in Table 2, the experimental formation water was configured according to the actual ionic composition of the formation water in the Tahe Oilfield. The experimental water was dyed with blue ink. The experimental temperature was 25 °C.

#### 3.2. Experimental instruments

Fig. 7 shows the instruments for displacement experiment in this study, including high-temperature dryer, displacement pump (with constant-speed and constant-pressure), flow controller, thermostat, foam generator, liquefied nitrogen cylinder, metering installation of liquid, intermediate vessel, six-way valve, and connection pipes, etc. The flow controller was used to control the gas injection rate and record the cumulative injection volumes of gas. The displacement pump was used to control the velocity of injection water. According to the experimental design, a CS200A gas flowmeter (measuring range was 0–50 mL/min, precision was 1%) and a 2PB-2020 advection pump (measuring range was 0.1–20 mL/min, accuracy was 1%) were selected.

#### 3.3. Experimental process

(1) The experimental scheme of 2D visual physical model of fractured-vuggy structure

In this study, the 2D visual physical model was used to carry out experimental research on foam flooding after water flooding and foam flooding after gas flooding. During the experiment, the

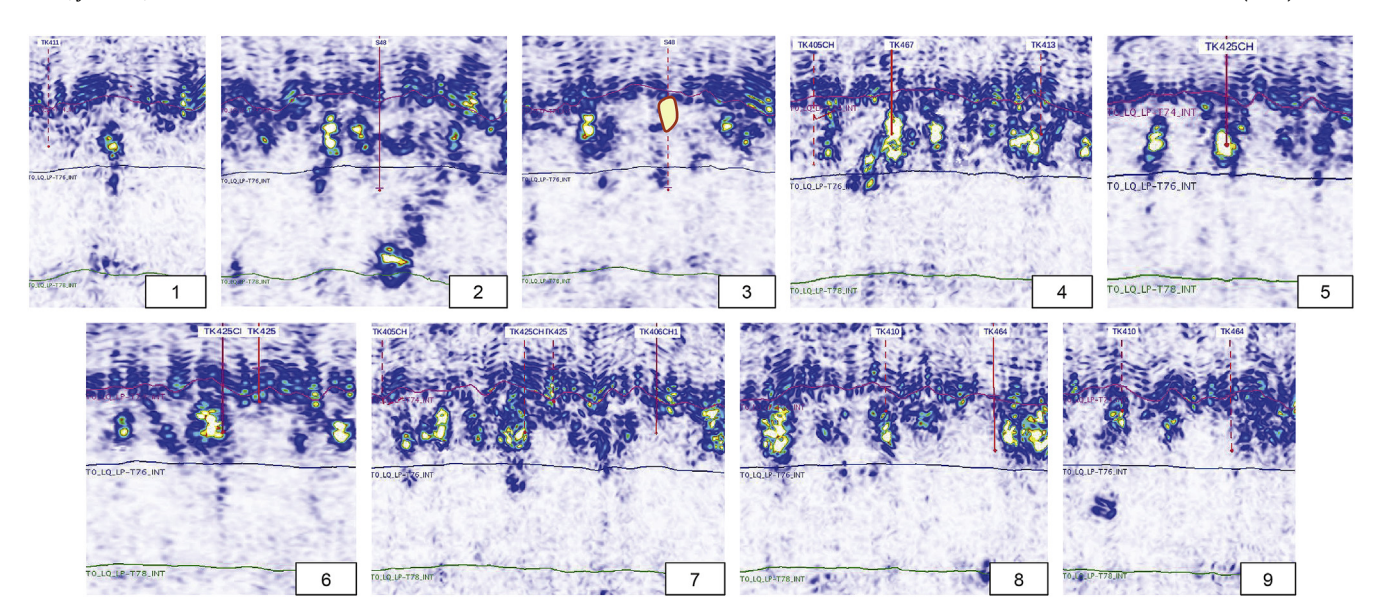


Fig. 5. Nine geological drawings of longitudinal sections of the TK425CH well group.

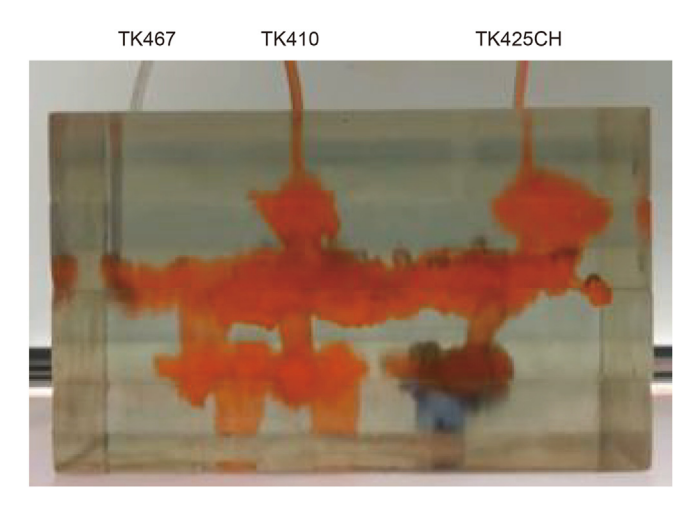


Fig. 6. The 3D visual physical model of TK425CH well group.

**Table 2** Ionic composition of formation water in the Tahe Oilfield.

Total salinity, mg/L	Ionic concentration, mg/L					
	Cl-	$Na^+ + K^+$	Ca <sup>2+</sup>	${\rm Mg}^{2+}$	SO <sub>4</sub> <sup>2-</sup>	HCO <sub>3</sub>
235828.4	146484.1	61385.4	25987.1	872.6	516.8	517.1

experimental temperature was 25 °C and the pressure was 0.1 MPa. The water injection rate was 2 mL/min, the gas injection rate was 5 mL/min, and the foam injection rate was 2 mL/min. Three kinds of displacement methods were designed to carry out experiments in this study (Fig. 8). The vertical displacement method was used to simulate the flow of fluid in the high angle fractured-vuggy structure. The longitudinal displacement method was used to simulate the flow of fluid in the longitudinal direction of the fractured-vuggy structure. The horizontal displacement method was used to simulate the flow of fluid in the horizontal direction of the fractured-vuggy structure. The specific experimental steps are as follows:

(a) The 2D visual physical model was saturated with oil.

- (b) Water injection was carried out with an water injection rate of 2 mL/min. Water injection was stopped until the water cut at the production channel reached 98%.
- (c) Gas injection was carried out at the injection channel, with an injection rate of 5 mL/min. Gas injection was stopped until gas channeling occurred at the production channel.
- (d) Foam injection was carried out at the injection channel with an injection rate of 2 mL/min. Foam injection was stopped until no oil was produced at the production channel.
- (e) The experimental process was recorded by a HD camera.
- (2) The experimental scheme of 3D visual physical model of fractured-vuggy carbonate reservoir

In this study, the 3D visual physical model was used to carry out the experimental study of water flooding, gas flooding, and foam flooding. The experimental temperature was 25  $^{\circ}$ C and the experimental pressure was 0.1 MPa. The water injection rate was 2 mL/min, the gas injection rate was 5 mL/min, and the foam injection rate was 2 mL/min. The specific experimental steps are as follows:

- (a) The 3D visual physical model was saturated with oil.
- (b) During the water flooding experiment, the water was injected into TK425CH well at a rate of 2 mL/min. The water flooding was stopped until the water cut of the production well reached 98%.
- (c) During the gas flooding experiment, the gas was injected into TK425CH well at a rate of 5 mL/min. The gas flooding was stopped until the gas channeling occurred at production wells.
- (d) During the foam flooding experiment, the foam was injected into TK425CH well at a rate of 2 mL/min. The foam flooding was stopped until no oil was produced at production wells.
- (e) The experimental process was recorded by a HD camera.

#### 4. Results and discussion

4.1. Experimental study of foam flooding in 2D visual physical model

The visual experimental results were provided in Section 4.1.

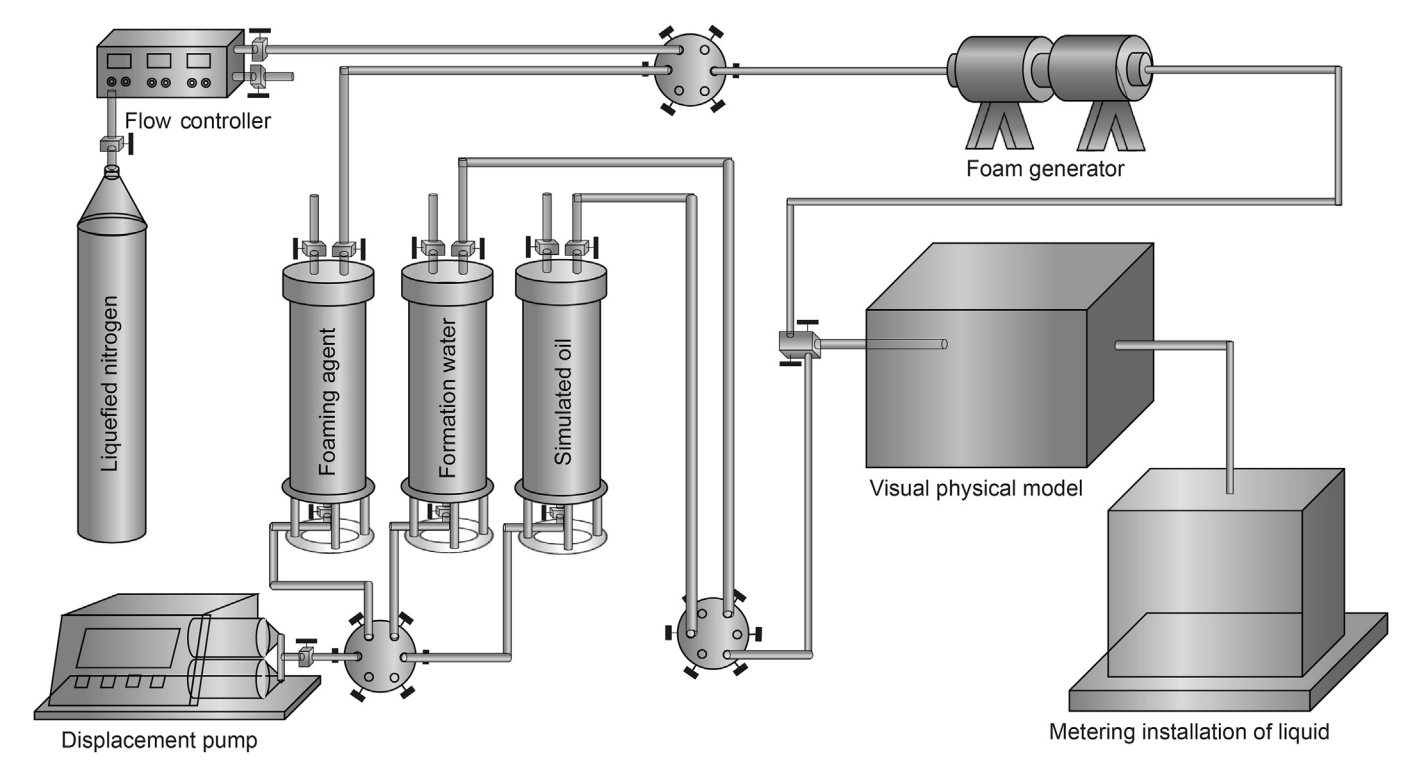


Fig. 7. The flow chart of foam flooding experiment.

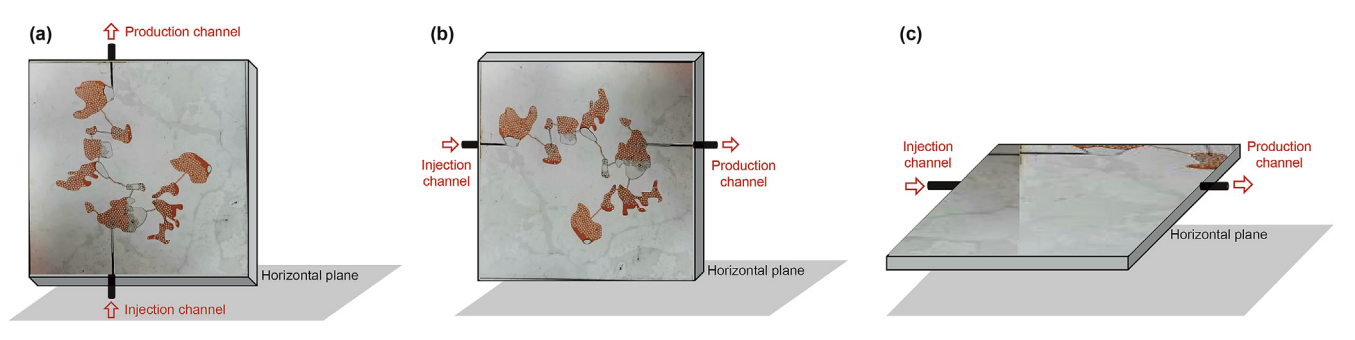


Fig. 8. Three experimental methods were used in the study, including vertical displacement (a), longitudinal displacement (b), and horizontal displacement (c).

Fig. 9 shows the experimental results of the 2D visual fractured model. Figs. 10–15 show the experimental results of the 2D visual vuggy model under different displacement methods. Figs. 16–18 show experimental results of the 2D visual fractured-vuggy model under different displacement methods. Figs. 19–21 show the recovery ratio of different experiments.

#### 4.1.1. Experiments of 2D visual fractured model

Gas flooding and foam flooding experiments were carried out with the fractured model. The results of different displacement methods are basically the same, and the experimental results are shown in Fig. 9. During the experimental process of gas flooding, gas entered the fracture ② along the small fracture after gas was injected into the fracture ③. Gas quickly flowed to the production channel along the fracture ②. After gas flooding, most parts of the fracture ③, only half of the fracture ①, and less than 1/3 of the fracture ③ were swept. Only a small part of small fractures was swept by gas. During the experimental process of foam flooding, foam moved forward along the fracture ① and entered small fractures with different apertures. Then foam entered the fracture

② and fracture ③ along small fractures. The subsequent foam did not flow into the production channel quickly along the fracture ②, but swept forward uniformly along the fractures with different apertures. Finally, the foam flooding displaced most of the oil in the fractures.

#### 4.1.2. Experiments of 2D visual vuggy model

Water flooding, gas flooding, and foam flooding experiments were carried out with three kinds of displacement methods using the vuggy model. The experimental results of the horizontal displacement are shown in Fig. 10. It is found that the displacement effect of water flooding and gas flooding in the filled vuggy structure was poor. Due to the different viscosity of fluids, fingering was easy to appear in the vuggy structure with strong heterogeneity. Fingering was extremely obvious in the process of gas flooding. After gas formed a dominant channel in the vuggy structure, a large amount of residual oil existed in the vuggy structure (as shown in Fig. 13a and b). The recovery ratio of water flooding was 62.7%, and the recovery ratio of gas flooding was 48.6%. Foam could effectively improve the mobility of oil and gas, it could plug the channelings

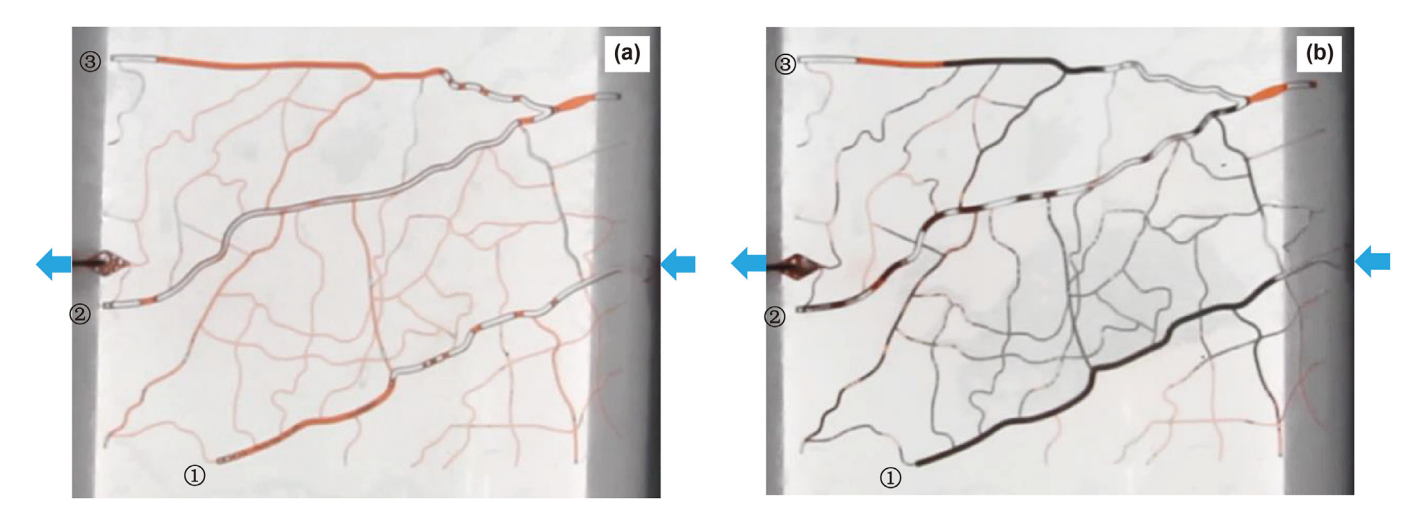


Fig. 9. The experimental results of displacement in fractured model. (a) Gas flooding; (b) Foam flooding.

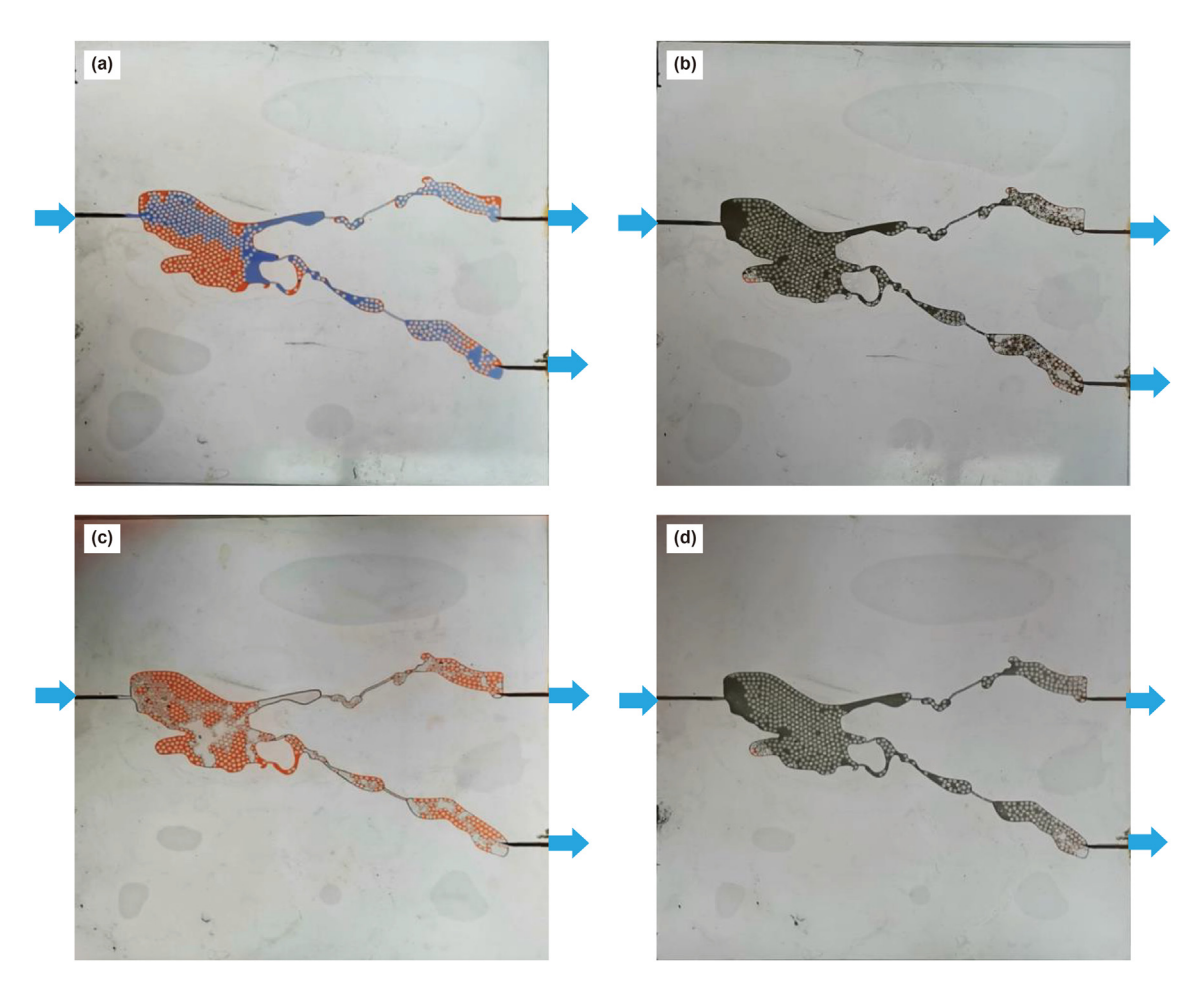


Fig. 10. The experimental results of displacement in the horizontal vuggy model. (a) Water flooding; (b) Foam flooding after water flooding; (c) Gas flooding; (d) Foam flooding after gas flooding.

and inhibit the low viscosity displacement media from advancing along the high permeability channel. Foam had a good displacement effect in vuggy structures (as shown in Fig. 13c), and the recovery ratio of foam flooding after water flooding and gas flooding was close to 95% (see Fig. 20).

The experimental results of the longitudinal displacement are

shown in Fig. 11. It is found that in the process of water flooding and gas flooding, gravity segregation was highly obvious in the longitudinal direction of the vuggy model. Since the density of water was higher than oil, the injected water could only sweep the lower part of the vuggy structure, but not the upper part of the vuggy structure. Due to the density of gas was lower than oil, gas flooding

was opposite to water flooding. The injected gas could only sweep the upper part of vuggy structure, but not the lower part of vuggy structure. Also, the microscopic displacement efficiency of water flooding and gas flooding was poor (as shown in Fig. 14a and b). The recovery ratio of water flooding was 51.2%, and the recovery ratio of gas flooding was 44.7%. Foam could effectively weaken the influence of gravity segregation in the longitudinal direction. The injected foam could simultaneously sweep the upper part and the lower part of vuggy structure, and the microscopic displacement efficiency of foam was high (as shown in Fig. 14c). Finally, the recovery ratio of foam flooding after water flooding and gas flooding was higher than 95% (see Fig. 20).

The experimental results of the vertical displacement are shown in Fig. 12. It is found that water flooding could simultaneously sweep multiple high-angle fractured-vuggy structures which are the common structure in the Tahe Oilfield. Due to the strong heterogeneity of filled fractured-vuggy structure, a large amount of microscopic residual oil still existed in the model after water flooding (as shown in Fig. 15a). The recovery ratio of water flooding in this model was 84.5%. The displacement effect of gas flooding in the high-angle fractured-vuggy structure was worse than that of water flooding. Due to the effect of gravity segregation, gas quickly channeling upward after it was injected into vugs. Since the dominant channel was formed in the fractured-vuggy structure, a large amount of residual oil could not be swept by gas in vugs (as shown in Fig. 15b). The displacement effect of gas was better in the fracture than that in the vug, but gas could sweep only one high-

angle fracture. The recovery ratio of gas flooding in this model was 23.4%. Foam could effectively decrease the mobility ratio, and the displacement effect of foam in high-angle fractured-vuggy structures was the best among these displacement experiments. The injected foam migrated upward uniformly in high-angle fractured-vuggy structures, and the residual oil in multiple high-angle fractured-vuggy structures was swept at the same time. The displacement effect of it was good in the filled vugs (as shown in Fig. 15c). The dominant channel formed by displacement media in the water flooding stage or gas flooding stage had little influence on foam flooding. Finally, the recovery ratio of foam flooding after water flooding was 96.8%, and the recovery ratio of foam flooding after gas flooding was 95.6% (see Fig. 20).

#### 4.1.3. Experiments of 2D visual fractured-vuggy model

Water flooding, gas flooding, and foam flooding experiments were carried out with three kinds of displacement methods using the fractured-vuggy model. The experimental results of horizontal displacement are shown in Fig. 16. It is found that the displacement effect of gas flooding in the horizontal fractured-vuggy structure was the worst among three experimental methods. Only a small amount of residual oil nearby the fractures was swept by gas (as shown in Fig. 16c). The recovery ratio of gas flooding in this model was only 25.1%. Water flooding swept the residual oil in the middle part of the connected fractures and vugs. But the residual oil around the corner and in the blind end of the fractured-vuggy structure was difficult to sweep (as shown in Fig. 16a). The recovery ratio of

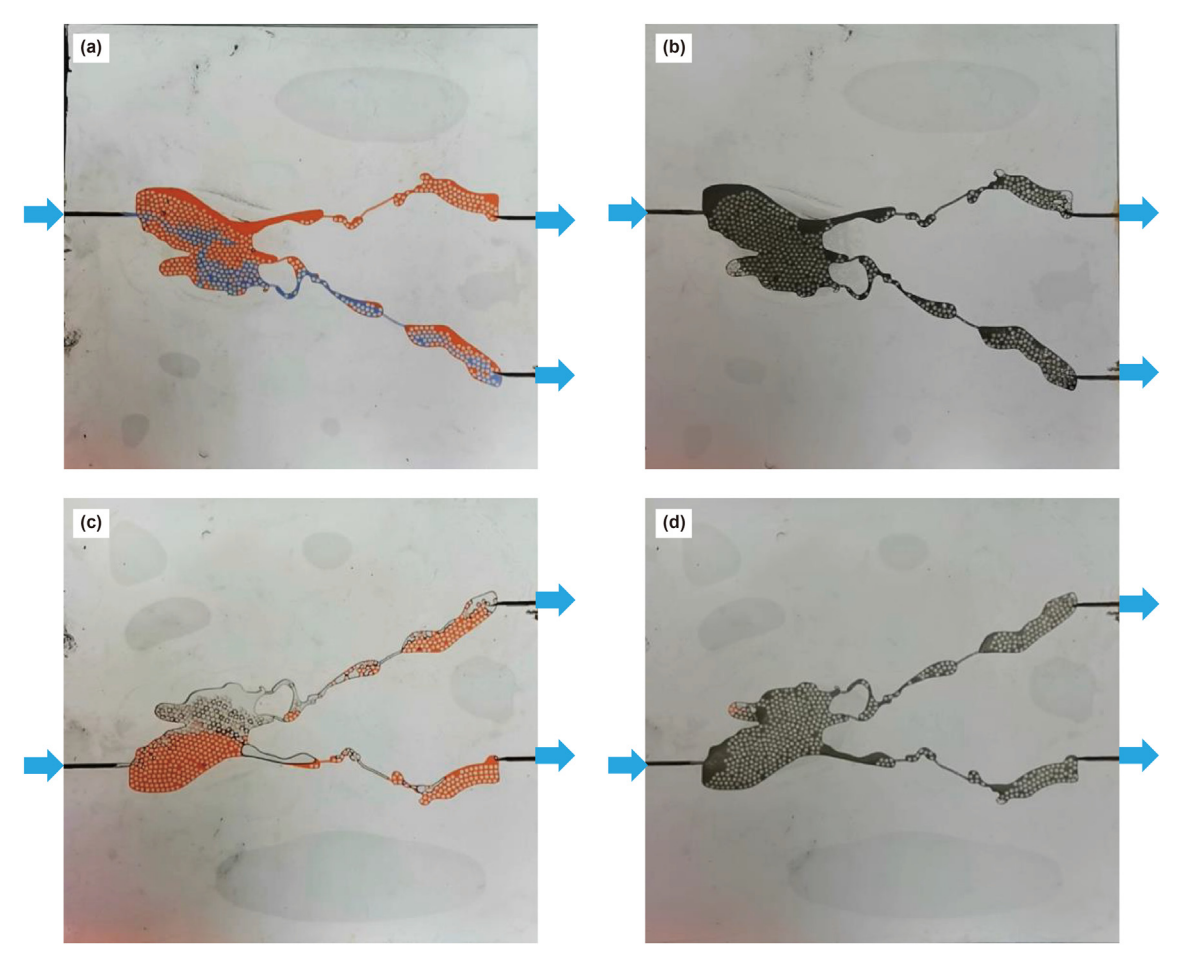


Fig. 11. The experimental results of displacement in the longitudinal vuggy model. (a) Water flooding; (b) Foam flooding after water flooding; (c) Gas flooding; (d) Foam flooding after gas flooding.

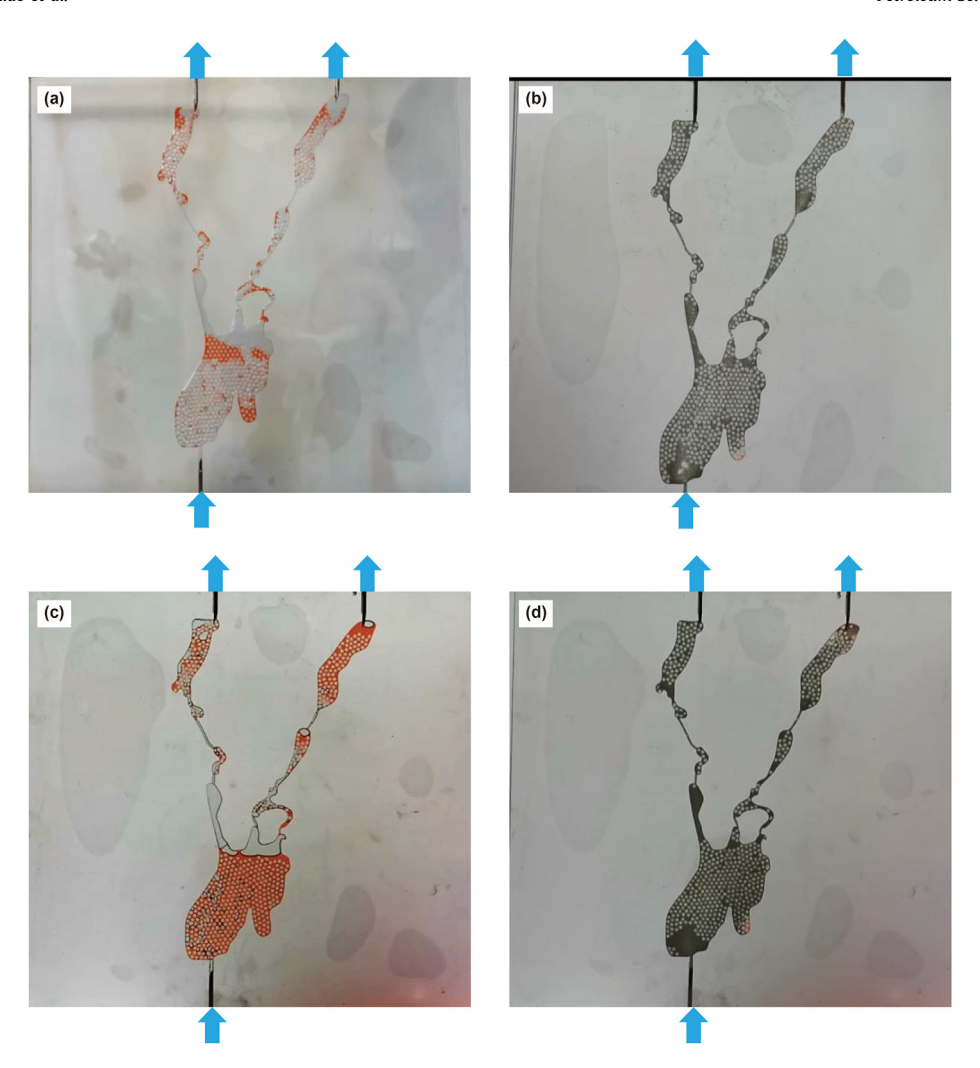


Fig. 12. The experimental results of displacement in the vertical vuggy model. (a) Water flooding; (b) Foam flooding after water flooding; (c) Gas flooding; (d) Foam flooding after gas flooding.

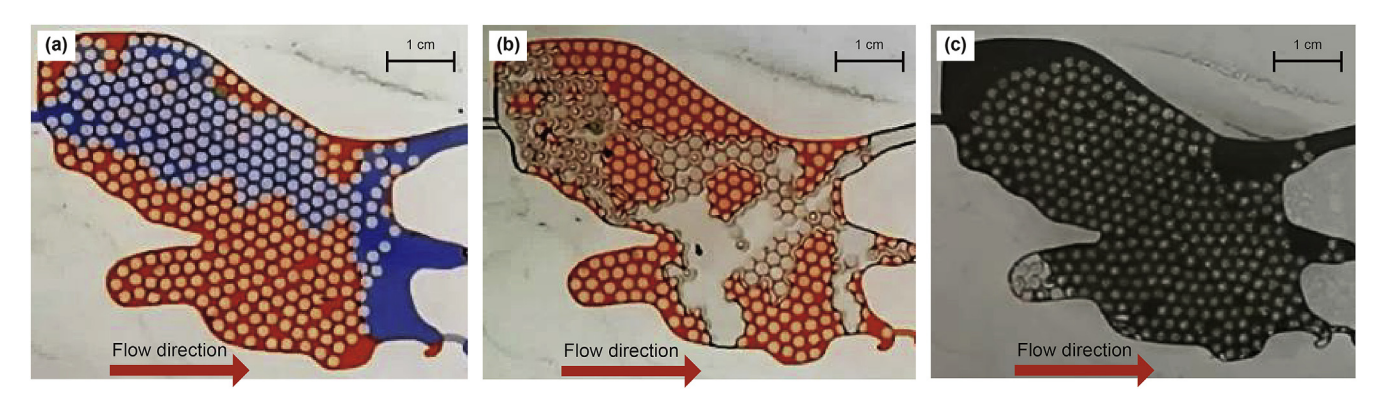


Fig. 13. The sweep volume after flooding in a single vuy of the horizontal vuggy model. (a) Water flooding; (b) Gas flooding; (c) Foam flooding.

water flooding in this model was 55.8%. By decreasing the mobility ratio of the displacement medium, foam effectively swept the residual oil around the corner (as shown in Fig. 16b, d). The recovery ratio of foam flooding was more than 60%. The residual oil was mainly concentrated in the blind end of the fractured-vuggy structure which could not be swept.

The experimental results of the longitudinal displacement and the vertical displacement are shown in Figs. 17 and 18. It is found that the injected gas had an obvious upward migration trend under the effect of gravity segregation. Gas effectively displaced the residual oil at the top of multiple longitudinal vugs which were continuously distributed along the horizontal direction, and formed a gas cap at the top of the fractured-vuggy structure (as shown in Fig. 17c). The recovery ratio of gas flooding in the longitudinal fractured-vuggy model was 31.2%. However, the swept volume of gas flooding was extremely small in the multiple vugs

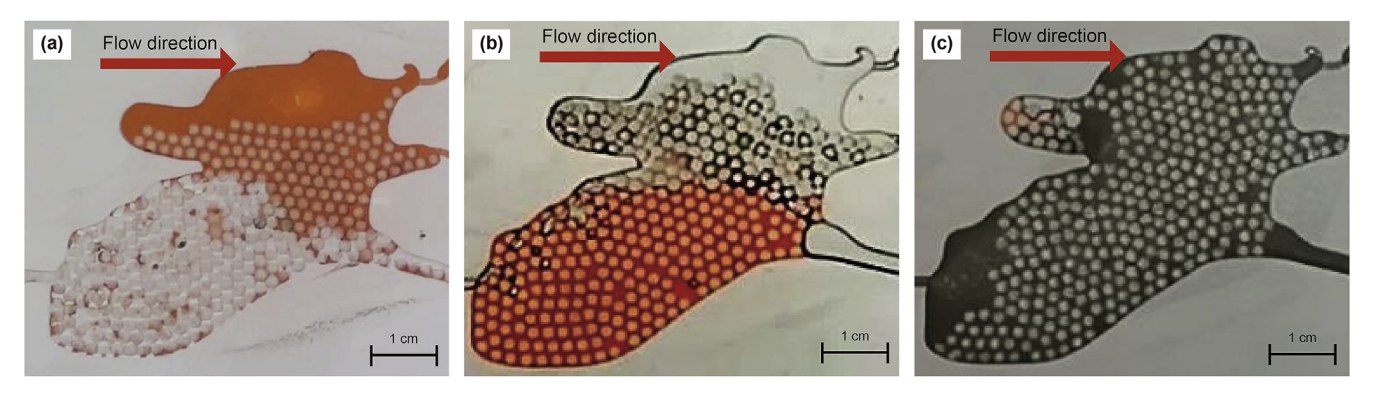


Fig. 14. The sweep volume after flooding in a single vuy of the longitudinal vuggy model. (a) Water flooding; (b) Gas flooding; (c) Foam flooding.

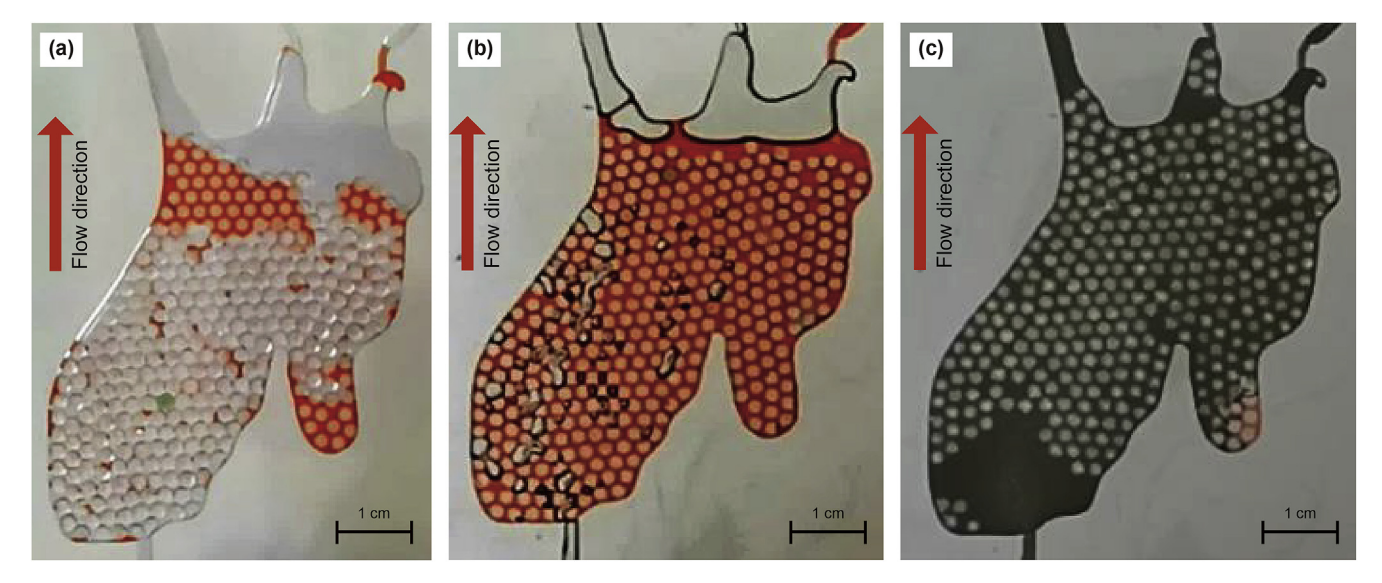


Fig. 15. The sweep volume after flooding in a single vuy of the vertical vuggy model. (a) Water flooding; (b) Gas flooding; (c) Foam flooding.

which were continuously distributed along the vertical direction. The injected gas quickly migrated upward along the fractures, resulted in a very small swept volume of each vug (as shown in Fig. 18c). The recovery ratio of gas flooding in the vertical fractured-vuggy model was 29.7% (see Fig. 21).

The injected water could only displace the residual oil below the oil—water interface in multiple longitudinal vugs which were continuously distributed along the horizontal direction (as shown in Fig. 17a). The recovery ratio of water flooding in the longitudinal fractured-vuggy model was 45.8%. The injected water could effectively displace most of the residual oil below the oil—water interface in the multiple vugs which were continuously distributed along the vertical direction (as shown in Fig. 18a). The recovery ratio of water flooding in vertical fractured-vuggy model was 52.5% (see Fig. 21).

The foam could effectively weaken the gravity segregation in the longitudinal direction, and the injected foam simultaneously swept the upper part and the lower part of fractured-vuggy structures (as shown in Fig. 17b, d, and 18b, d). The maximum recovery ratio of foam flooding in this model reached 66% (see Fig. 21).

## 4.2. Analysis on the sweep mechanism in fractured-vuggy structures

4.2.1. Sweep mechanism of foam in complex fracture network
Foam has a good sweep effect on single fracture with different

apertures, but complex fracture networks were formed by connected fractures in fractured-vuggy reservoirs. Thus, experiments of gas flooding and foam flooding were conducted in the complex fractured model to reveal the sweep mechanism of gas and foam. Based on the Boussinesq equation, the calculation equation of liquid flow in unit length fracture was obtained (Gee and Gracie, 2022). It can be inferred from this equation that the fluid in the fracture can flow only when the pressure gradient is positive.

$$q = \frac{b^3}{12\mu} \frac{\mathrm{d}P}{\mathrm{d}x} \tag{1}$$

where q is the flow rate of fluid in per unit length of fracture,  $m^2/s$ ; b is the fracture width, m;  $\mu$  is the fluid viscosity, Pa s; dP/dx is the pressure gradient, Pa/m.

Fig. 22 shows the experimental results of gas flooding and foam flooding in the fractured model. It is found that gas migrated forward along large-aperture fractured channels in the complex fracture network, and the sweep volume of small-aperture fractures was small. However, foam flooding possessed a good swept ability in the complex fracture network, and could displace most small-aperture fractures. Due to low viscosity of gas, the pressure gradient decreased slowly when gas flowed through fractures. This resulted that the pressure difference between B and D was not enough to overcome the flow resistance between B and D, so the gas could not enter the fracture and displace the residual oil

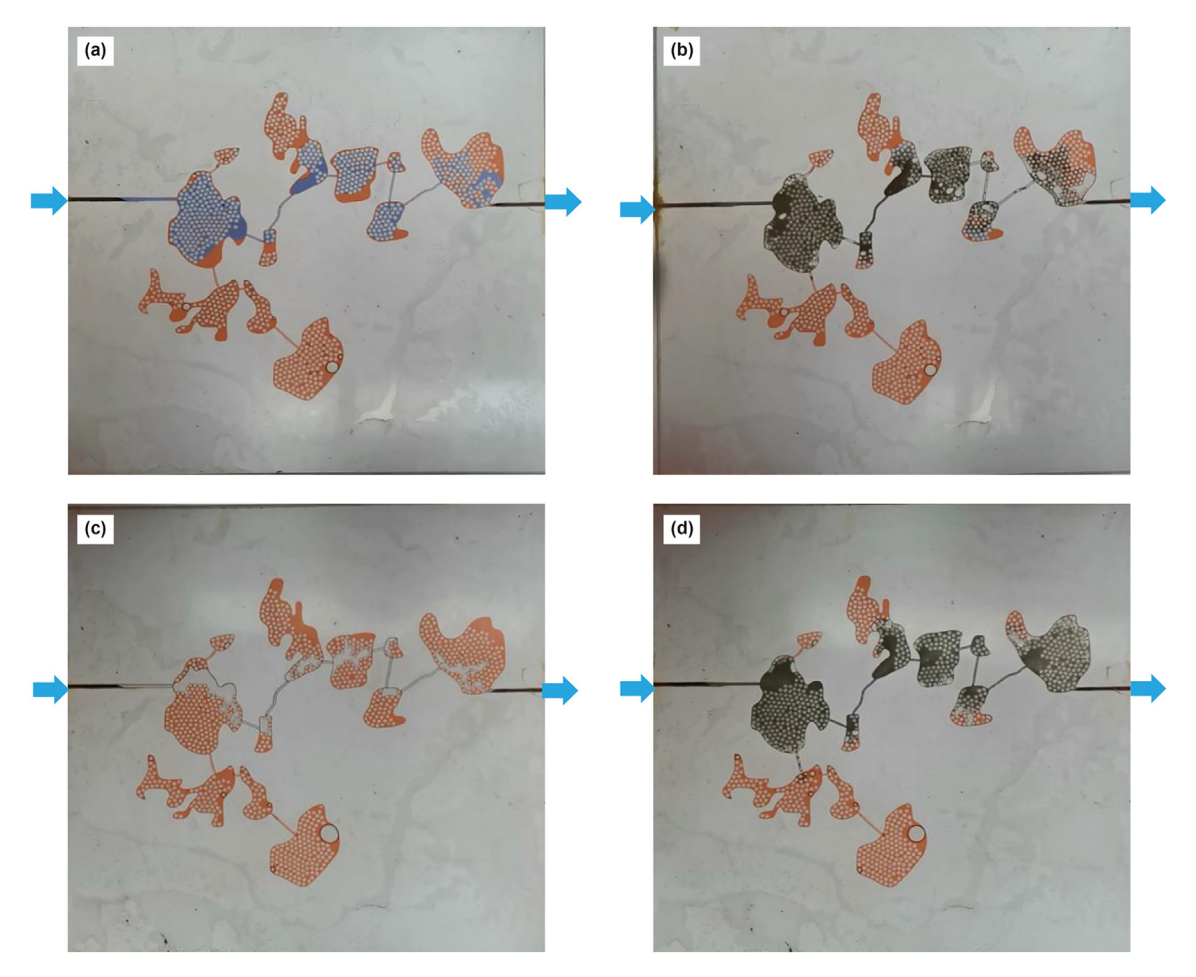


Fig. 16. The experimental results of displacement in horizontal fractured-vuggy model. (a) Water flooding; (b) Foam flooding after water flooding; (c) Gas flooding; (d) Foam flooding after gas flooding.

between B and D (as shown in Fig. 22b). The viscosity of foam was higher than gas and the superposition of Jamin effect was serious, which caused the pressure decreased rapidly when gas flowed through fractures. This resulted that the pressure difference between B and D was enough to overcome the flow resistance between B and D. Foam could enter the fracture and displace the residual oil between B and D (as shown in Fig. 22c). Foam effectively swept the complex fracture network in the fractured model for the same reason. The recovery ratio of gas flooding in this model was only 36.4%, but the recovery ratio of foam flooding in this model was 82.3%. Foam expanded the sweep volume and improved the oil recovery ratio in fractured-vuggy structures.

Theoretically, the increase in the viscosity of the foam results in an increase in pressure under the ideal condition of infinite injection pressure. Therefore, all connected fractures in fractured-vuggy reservoir can be swept. But the swept volume of foam flooding in the fractured-vuggy reservoir is not as good as the experimental results, due to the injection pressure of the oilfield is limited, the reservoir condition is complex, and the flow resistance of fluid is affected by many factors. The effect of foam flooding in fractures can be improved by increasing the strength of foam and enhancing the stability of foam.

#### 4.2.2. Sweep mechanism of foam in vugs

During the foam flooding experiment in the fractured-vuggy model, it is found that whether the foam can displace the oil in vugs mainly depends on the relationship between the driving force and the flow resistance of fluid. Foam could displace the oil in vugs when the driving force is higher than the flow resistance. Fig. 23 shows the process of foam displaced residual oil in the vug.

The driving force of foam flooding in the vug is represented by the pressure difference between the injection channel and the output channel:

$$P_{\text{drive}} = P_{\text{in}} - P_{\text{out}} \tag{2}$$

The gravity caused by the density difference between foam and oil is defined as:

$$\Delta P_{\rm m} = \left(\rho_{\rm o} - \rho_{\rm f}\right) gh \tag{3}$$

The flow resistance of foam flooding in the vug including starting pressure ( $P_f$ ) caused by friction between oil, foam and rocks and the capillary force ( $P_c$ ) of the oil and water at the outlet end in the fracture.

$$P_{\rm c} = \frac{2\sigma {\rm cos}\theta}{w} \tag{4}$$

where  $P_{\rm in}$  is the injection pressure, Pa;  $P_{\rm out}$  is the output pressure, Pa;  $\rho_{\rm o}$  is the density of oil, kg/m<sup>3</sup>;  $\rho_{\rm f}$  is the density of foam, kg/m<sup>3</sup>; g is the gravitational acceleration;  $\sigma$  is the interfacial tension between foam and oil, mN/m;  $\theta$  is the contact angle between foam and facture surface, degree; w is the width of fracture, m;  $P_{\rm f}$  is the starting pressure caused by friction between oil, foam and rocks, Pa.

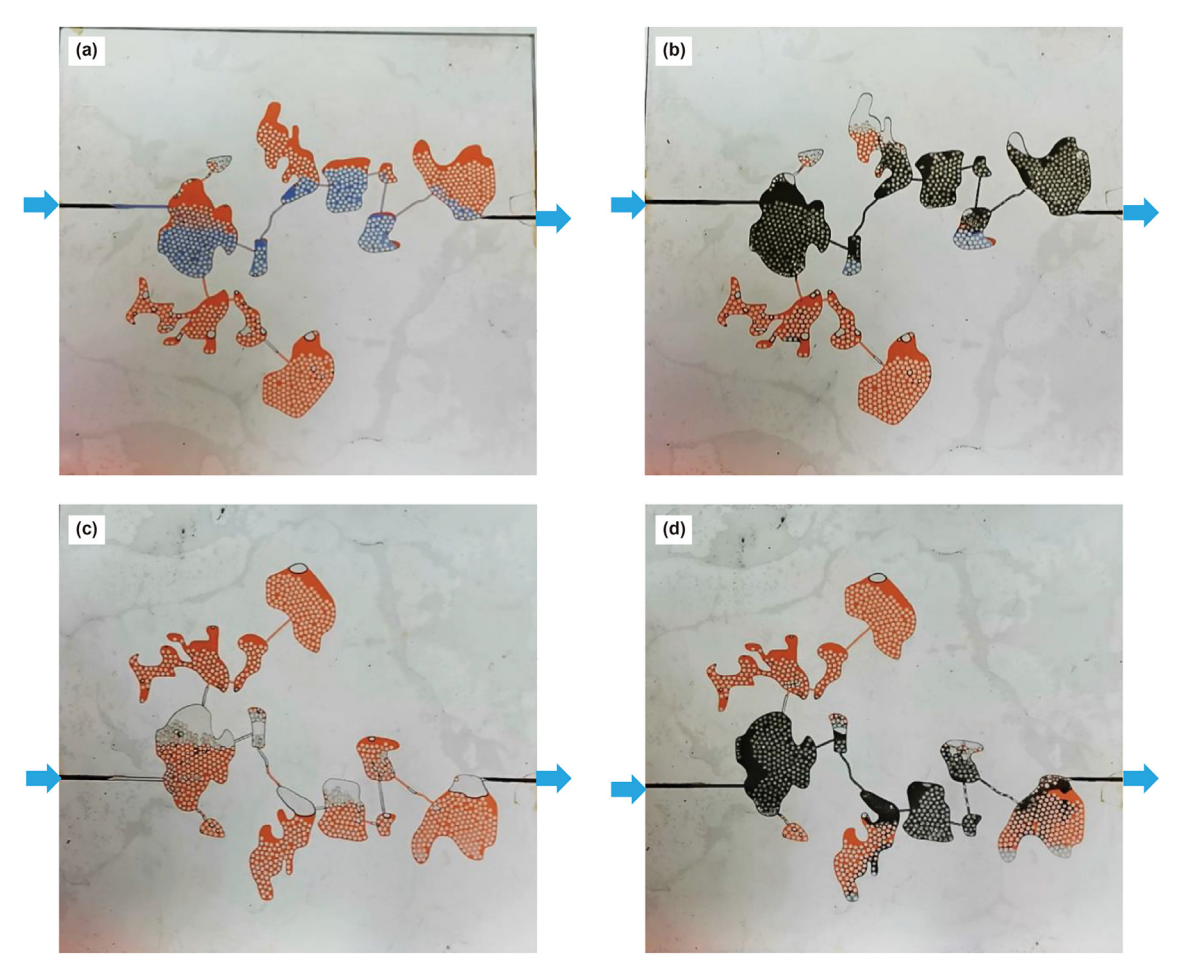


Fig. 17. The experimental results of displacement in the longitudinal fractured-vuggy model. (a) Water flooding; (b) Foam flooding after water flooding; (c) Gas flooding; (d) Foam flooding after gas flooding.

The foam sweep ability in vugs is defined as factor N, which is used to judge whether the residual oil in a vug can be sweep by the foam or not.

$$N = \frac{P_{\text{drive}} + \Delta P_{\text{f}}}{P_{\text{f}} + P_{\text{c}}} = \frac{(P_{\text{in}} - P_{\text{out}}) + \left(\rho_{\text{o}} - \rho_{\text{f}}\right)gh}{P_{\text{f}} + \frac{2\sigma\cos\theta}{w}}$$
(5)

N > 1 indicates that the driving force of foam in the vug is bigger than the flow resistance, so the foam can displace the oil in the vug. Otherwise, the oil in the vug cannot be swept. Eq. (5) indicates that the smaller the density of foam is, the smaller the interfacial tension between foam and oil is, and the more conducive it is to sweep the vug by foam. Therefore, the recovery ratio of foam in vugs can be improved by reducing the density of foam and the interfacial tension between foam and oil.

# 4.3. Experimental study of foam flooding in 3D visual physical model

#### 4.3.1. Water flooding in 3D visual physical model

The reservoir of TK425CH well group is a typical fractured-vuggy reservoir. Two main underground river channels exist between TK425CH well and TK467 well. TK467 well is located on one of the underground rivers, TK410 well and TK425 well are located in vugs. The 3D visual physical model was made according to this well group. Water flooding was carried out in this model and the experimental results were shown in Fig. 24. The injected water

migrated along the underground river to TK410 well after it was injected into TK467 well. The subsequent injected water gradually moved on, and the water cone phenomenon occurred in TK410 well after water entered the vug at the bottom of TK410 well. But the other underground river was not effectively swept by water flooding. In order to simulate the intrusion of bottom water, water was injected from the bottom of the model during water flooding. The bottom water gradually migrated upward and entered the underground river. Experiments shown that the water flooding could only displace the residual oil in the lower part of the fractured-vuggy and underground river structure, and a large amount of residual oil was concentrated in other high parts. The recovery ratio of water flooding in 3D visual physical model was 39.7%.

#### 4.3.2. Gas flooding in 3D visual physical model

Gas was injected through the TK425CH well into the 3D visual physical model during the gas flooding (see Fig. 25). Gas migrated along the different underground river from water flooding after it was injected into the model. The injected gas displaced the residual oil in the vug around the TK425CH well first, and then migrated into the underground river. Gas flowed along the underground river channel in the direction of TK425CH-TK467, which led to the gas channeling occurred in the TK467 well first. The subsequent gas migrated to the TK410 well along the underground channel. Gas displaced residual oil in the vug at the bottom of TK410 well. A gas cap was formed to replace the attic oil at the top of vug, but the

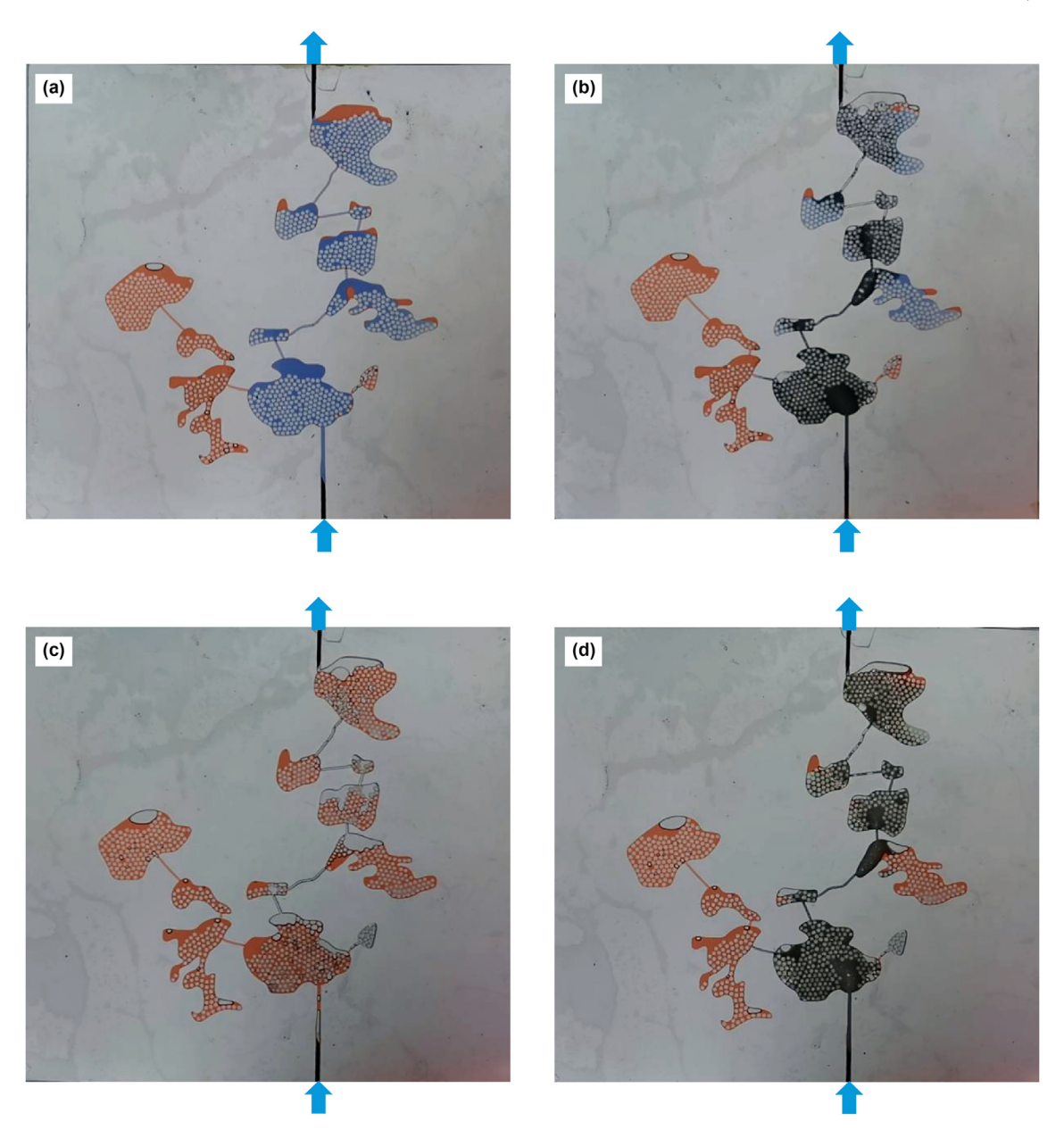


Fig. 18. The experimental results of displacement in the vertical fractured-vuggy model. (a) Water flooding; (b) Foam flooding after water flooding; (c) Gas flooding; (d) Foam flooding after gas flooding.

residual oil at the lower part of the vug was not effectively displaced. The dominant gas channeling was formed in the direction of TK425CH-TK467, and the recovery ratio of gas flooding in this model was 68.2%.

#### 4.3.3. Foam flooding in 3D visual physical model

Foam was injected through the TK425CH well into the 3D visual physical model during the foam flooding (see Fig. 26). The swept volume of foam flooding was best compared with water flooding and gas flooding. The injected foam had a good swept effect on the vug at the bottom of TK425CH well. Foam increased the flow resistance and improved the mobility ratio after it migrated into underground river. Foam inhibited the subsequent fluid from rushing along the channeling channel of water flooding or gas flooding and effectively swept two different underground rivers at the same time. The recovery ratio of foam flooding in this model

was 79.6%. This experimental result proved that foam could inhibit the water and gas channeling, control the flow velocity and flow direction of subsequent fluids in fractured-vuggy reservoirs, and displace uniformly in multiple directions at the same time. It could not only expand the swept volume, but also improve oil displacement efficiency in fractured-vuggy reservoirs.

Gas flooding improved recovery ratio by 28.5% after water flooding in the 3D visual physical model (see Fig. 27). The average recovery ratio of water flooding in No. 4 district of the Tahe Oilfield was 37.43%, and the recovery ratio of gas flooding was 30.3%, which is basically consistent with experimental results in the 3D visual physical model. After 0.4 PV foam was injected into the 3D visual physical model, foam flooding improved recovery ratio by 11.4% after gas flooding. This indicates that foam flooding can be taken in the fractured-vuggy reservoirs of the Tahe Oilfield. By applying foam flooding in TK425CK well to sweep the residual oil in the

Y.-C. Wen, J.-R. Hou, X.-L. Xiao et al. Petroleum Science 20 (2023) 1620–1639

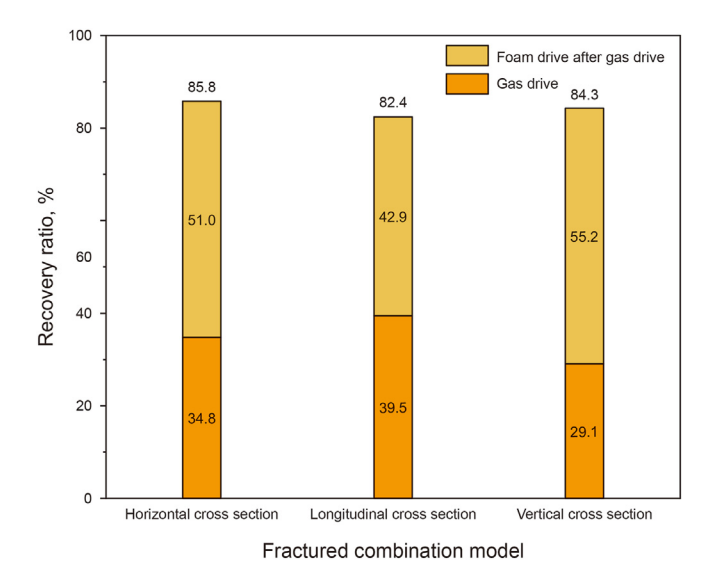


Fig. 19. The recovery ratio of different experimental methods in fractured models.

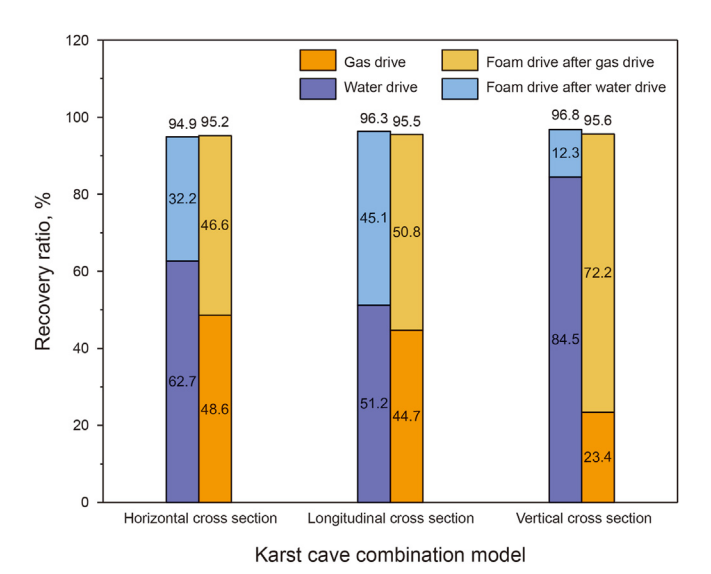


Fig. 20. The recovery ratio of different experimental methods in vuggy model.

reservoir, it is estimated that the recovery ratio can be improved by more than 10%.

# 4.4. The distribution of residual oil after foam flooding in fractured-vuggy reservoirs

During the water flooding experiment of the visual physical model, it is observed that the residual oil of fractured-vuggy carbonate reservoir could be divided into four types of microscopic residual oil and four types of macroscopic residual oil.

Microscopic residual oil included: oil film (Micro-1), residual oil in pores and throats (Micro-2), residual oil in the corners (Micro-3), and residual oil at the blind end vugs (Micro-4). Oil film (Micro-1) refers to the residual oil adsorbed on the rock wall due to the wettability of the rock, which is difficult to be completely stripped off by the displacement media. The thickness of oil film is usually less than 1 mm. Residual oil in pores and throats (Micro-2) refers to the residual oil in the connected pores and throats between rock particles in the filled fractured-vuggy structure. The diameter of

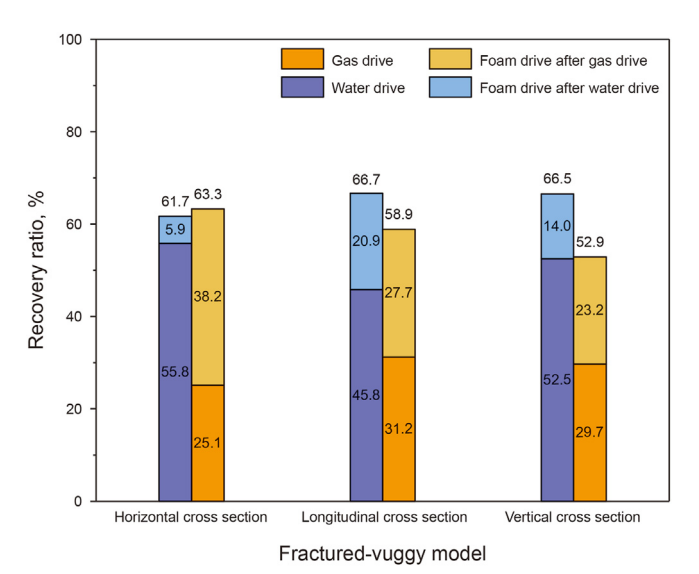


Fig. 21. The recovery ratio of different experimental methods in fractured-vuggy models.

pores and throats is usually less than 1 mm. The formation of this type of residual oil is mainly due to the difference in mobility ratio between the injected medium and the crude oil. The crude oil is unable to be completely displaced by displacement media in the pore and throat. Residual oil in the corners (Micro-3) refers to the residual oil at the edge of the irregular vugs. Residual oil in the blind end vugs (Micro-4) refers to the residual oil in the fractured-vuggy structure with only one connected fracture channel (the width of fractures is usually less than 1 cm). The formation of residual oil in the corners (Micro-3) and the blind end vugs (Micro-4) was mainly caused by the complex geometric structure of fractured-vuggy reservoirs, which caused the residual oil unable to be sweep by conventional displacement media.

Macroscopic residual oil included: attic oil (Macro-1), residual oil shielded by channeling (Macro-2), bypassed residual oil in connected fractured-vuggy structure (Macro-3), and residual oil disturbed by bottom water (Macro-4). Attic oil (Macro-1) is the residual oil in the high part of fractured-vuggy structures, which is difficult to be swept by water flooding, but can be effectively swept by gas flooding. When the displacement medium migrates across multiple fractured-vuggy channels, channeling is extremely easy to form in one of these channels, and the rest of these channels cannot be effectively swept. The residual oil in these channels is defined as residual oil shielded by channeling (Macro-2). After the channeling is formed in the fractured-vuggy structure, the fractures and vugs around the channeling are difficult to be effectively swept by the displacement medium. The bypassed residual oil in connected fractured-vuggy structure (Macro-3) is formed in this way. The fractured-vuggy structures are complex, and the oil-water interface is not consistent in different fractured-vuggy structures. Due to water drive and the invasion of bottom water, some part of the fractured-vuggy structures is submerged by the water before it is swept. The residual oil in this kind of fractured-vuggy structure is defined as residual oil disturbed by bottom water (Macro-4).

### 4.4.1. The distribution of microscopic residual oil in fractured-vuggy reservoirs

(a) The distribution of microscopic residual oil after water flooding

Y.-C. Wen, J.-R. Hou, X.-L. Xiao et al. Petroleum Science 20 (2023) 1620—1639

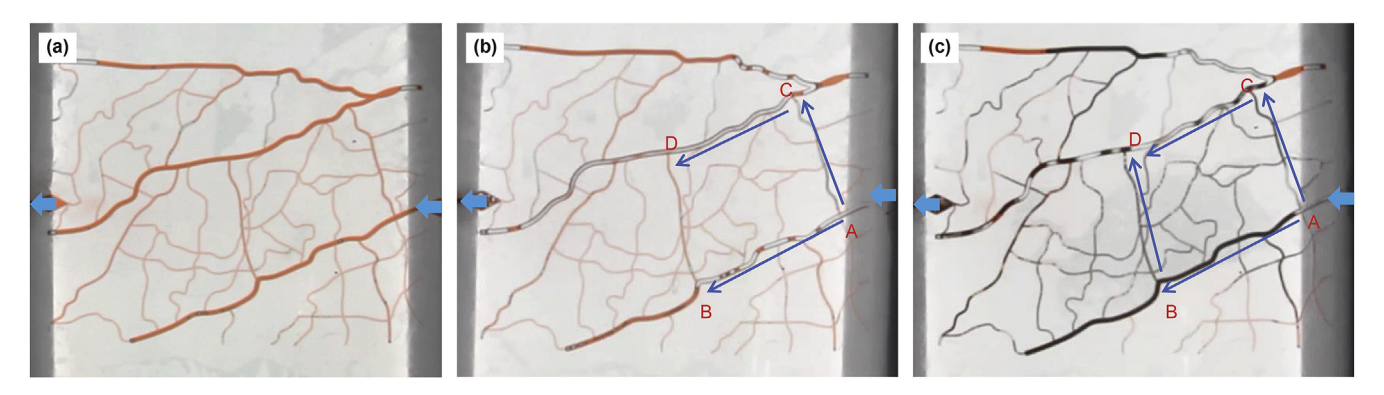


Fig. 22. Oil distribution before swept (a), residual oil swept by gas (b) and foam (c) in the complex fracture network.

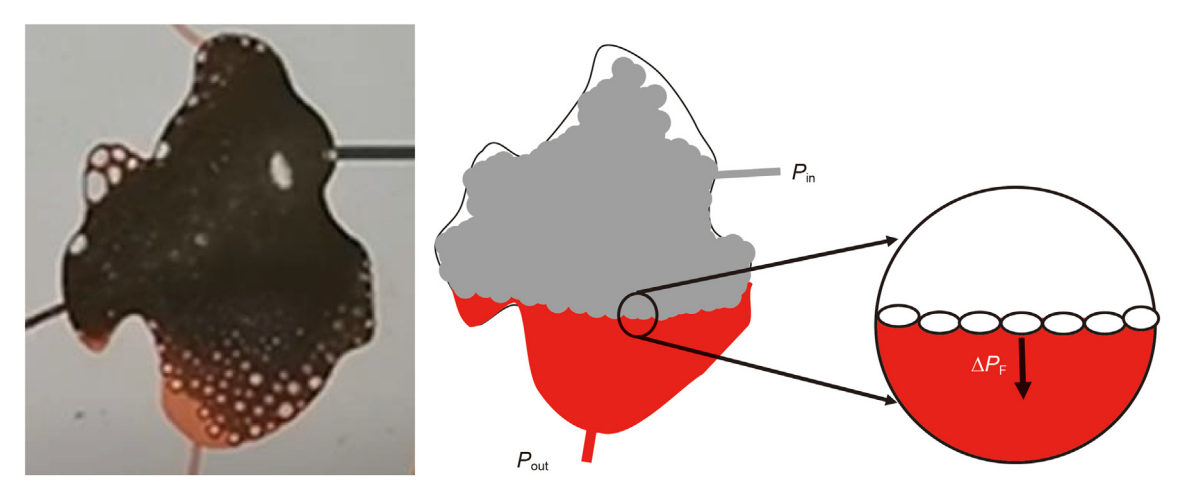


Fig. 23. Residual oil swept by foam in the vug.

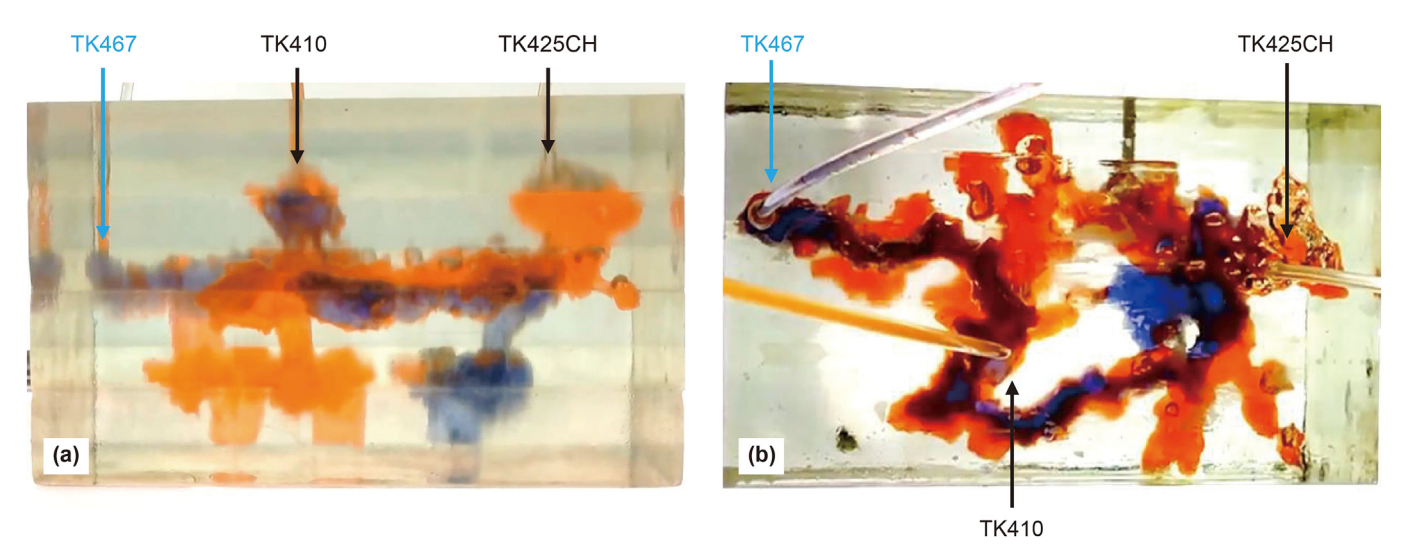


Fig. 24. Schematic of water flooding in the 3D visual physical model. (a) Front view; (b) Top view.

Fig. 28 shows the experimental results of water flooding in the 2D visual physical model of fractured-vuggy structure. The existence of filled medium enhanced the heterogeneity of fractured-vuggy structure, and resulted in a low microscopic displacement efficiency of water flooding. Four types of microscopic residual oil still existed in fractured-vuggy reservoirs after water flooding,

including Micro-1, Micro-2, Micro-3 and Micro-4.

(b) The distribution of microscopic residual oil after gas flooding

Fig. 29 shows the experimental results of gas flooding in the 2D visual physical model of fractured-vuggy structure. Due to the

Y.-C. Wen, J.-R. Hou, X.-L. Xiao et al. Petroleum Science 20 (2023) 1620—1639

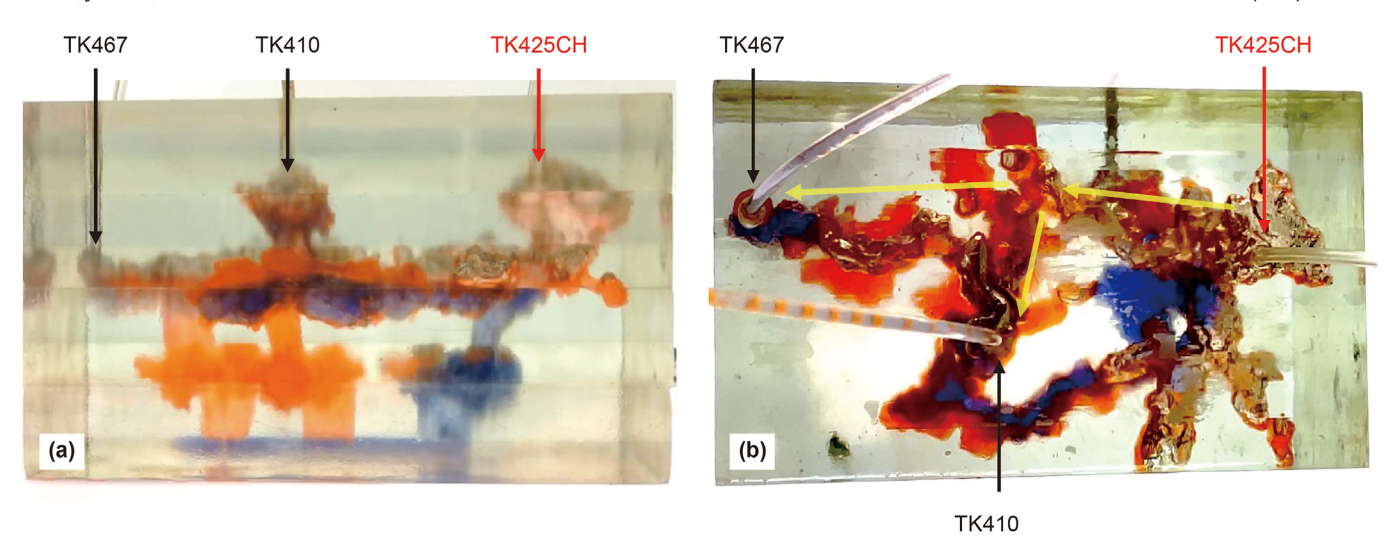


Fig. 25. Schematic of gas flooding in the 3D visual physical model. (a) Front view; (b) Top view.

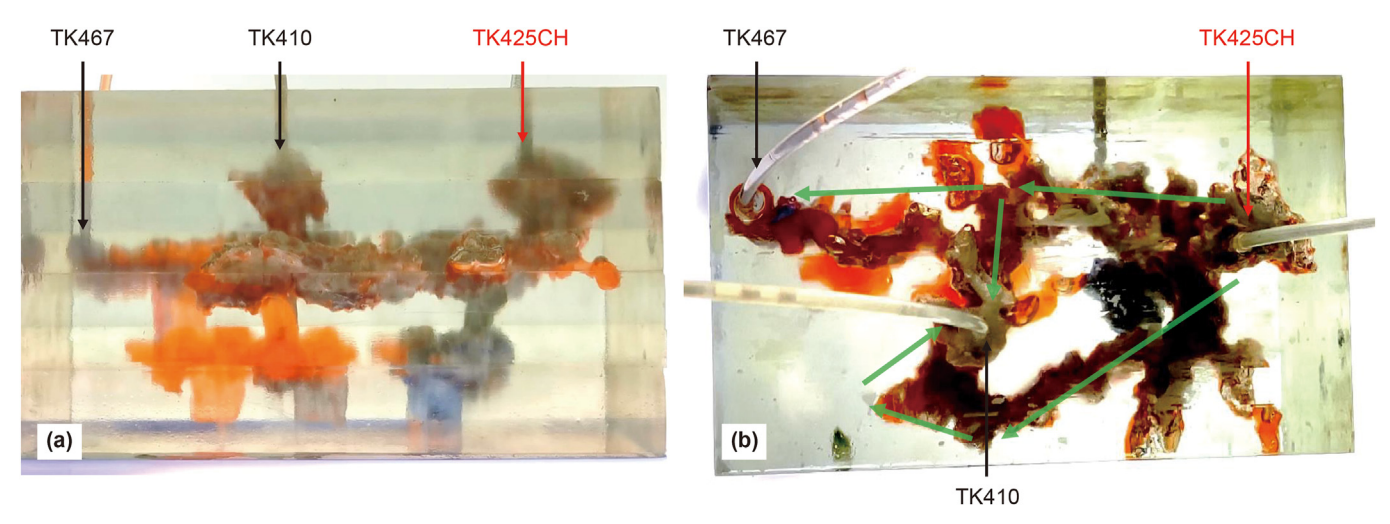
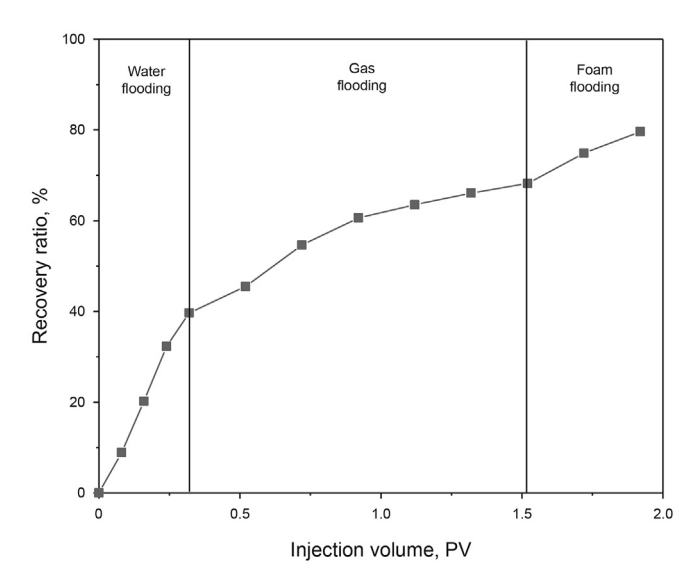


Fig. 26. Schematic of foam flooding in the 3D visual physical model. (a) Front view; (b) Top view.

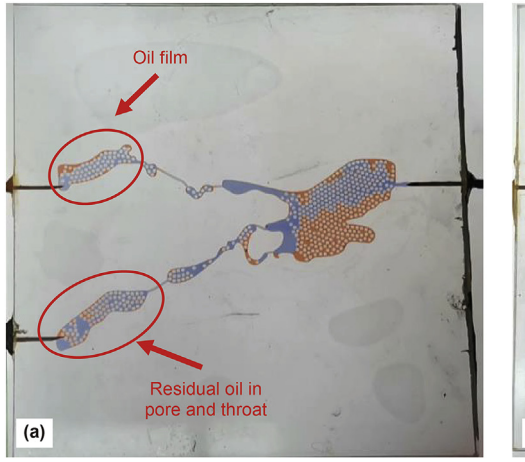


**Fig. 27.** Recovery ratio versus injection volume in displacement experiment of the 3D visual physical model.

influence of viscosity difference, fingering was easy to occur in fractured-vuggy structures, and gas channeling was easy to form along the high permeability channel. The microscopic displacement efficiency of gas flooding was extremely low. Four types of microscopic residual oil still existed in fractured-vuggy reservoirs after gas flooding, including Micro-1, Micro-2, Micro-3 and Micro-4.

# (c) The distribution of microscopic residual oil after foam flooding

Fig. 30 shows the experimental results of foam flooding in the 2D visual physical model of fractured-vuggy structure. Foam could effectively improve the mobility ratio, plug the dominant channels of water and gas, control flow rate and divert flow direction, and expand the sweep volume. It could effectively sweep the residual oil in pores and throats. The surfactant contained in the foam liquid could be adsorbed on the rock surface and change the wettability of the surface from oil-wet to water-wet. It could strip out the oil film on the rock surface. Only two types of microscopic residual oil still existed in fractured-vuggy reservoirs after foam flooding, including Micro-3 and Micro-4.



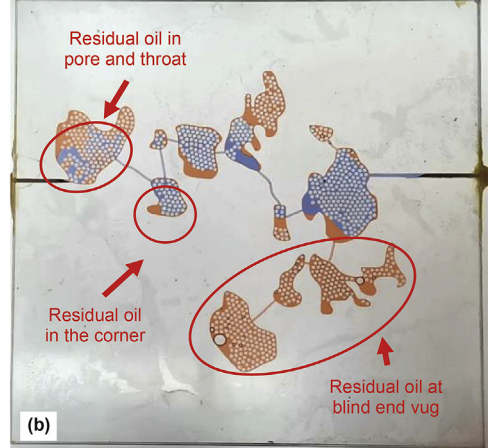
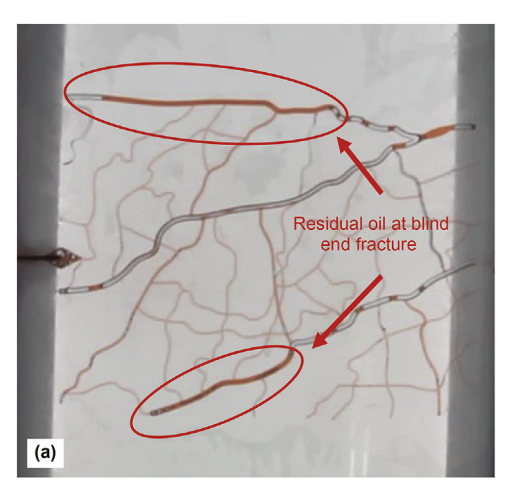


Fig. 28. The distribution of residual oil after water flooding in the 2D visual physical model.



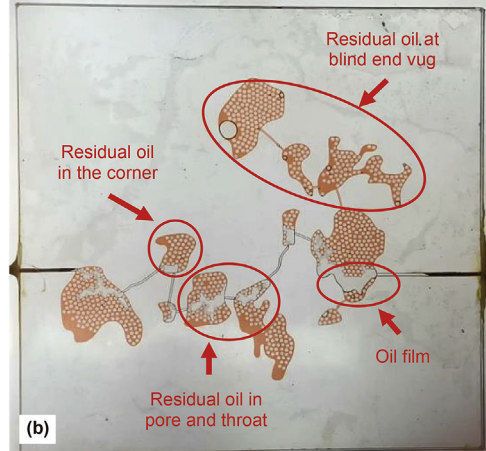
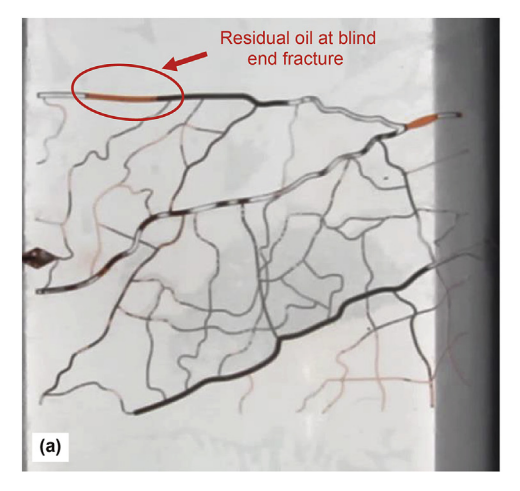


Fig. 29. The distribution of residual oil after gas flooding in the 2D visual physical model.

- 4.4.2. The distribution of macroscopic residual oil in fractured-vuggy reservoirs
  - (a) The distribution of macroscopic residual oil after water flooding

Fig. 31 shows the experimental results of water flooding in the 3D visual physical model of fractured-vuggy reservoir. Water channeling was formed in one of the underground rivers after water flooding, and a large number of residual oil (Macro-3) existed in this channel. The other underground river was not swept by



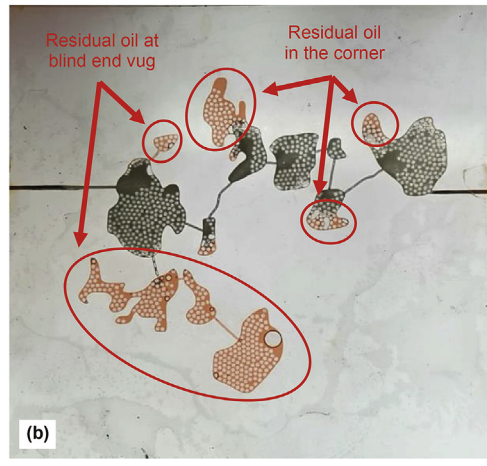
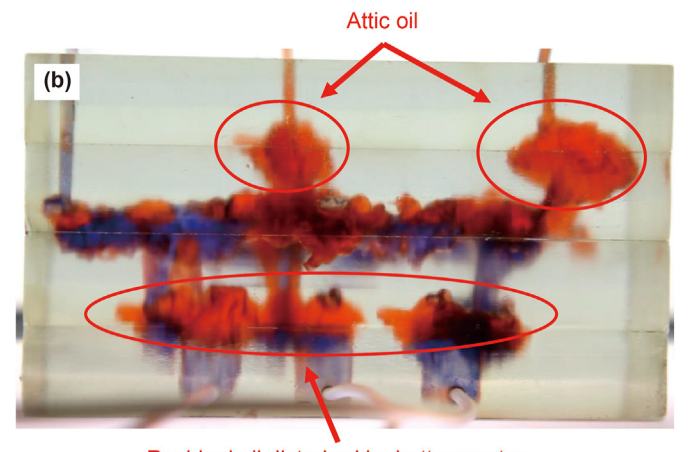


Fig. 30. The distribution of residual oil after foam flooding in the 2D visual physical model.

Y.-C. Wen, J.-R. Hou, X.-L. Xiao et al. Petroleum Science 20 (2023) 1620—1639

# Residual oil shielded by channeling (a)



Bypassed residual oil in connected fracture-vuggy structure

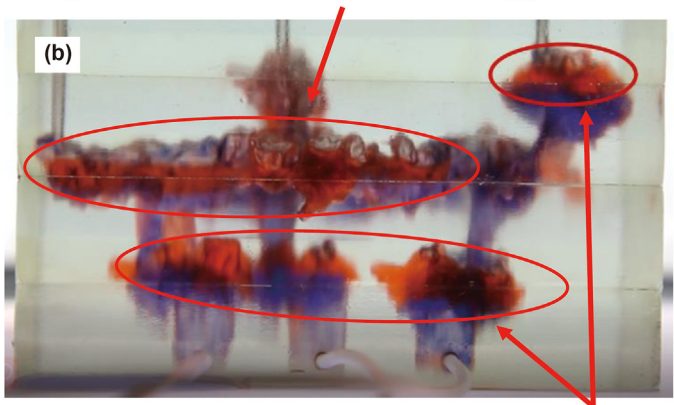
Residual oil disturbed by bottom water

Fig. 31. The distribution of residual oil after water flooding in the 3D visual physical model.



Residual oil shielded by channeling

#### Bypassed residual oil in connected fracture-vuggy structure



Residual oil disturbed by bottom water

Fig. 32. The distribution of residual oil after gas flooding in the 3D visual physical model.

water flooding, and a large number of residual oil (Macro-2) existed in this channel. The top vug of the reservoir was not swept by water flooding and a large number of attic oil (Macro-1) existed in these vugs. Some vugs at the lower part of fractured-vuggy reservoir were submerged by the bottom water, and a large amount of residual oil (Macro-4) was formed in these vugs.

(b) The distribution of macroscopic residual oil after gas flooding

Fig. 32 shows the experimental results of gas flooding in the 3D visual physical model of fractured-vuggy reservoir. A gas channeling was formed in one of the underground river channels after gas flooding, and a large number of residual oil (Macro-3) existed in this channel. The other underground river was not swept by gas flooding, and there is a large number of residual oil (Macro-2) existed in this channel. Gas flooding effectively swept the attic oil in top vugs of the reservoir, but a large amount of residual oil (Macro-4) still existed in the lower part of fractured-vuggy reservoir due to the existence of bottom water.

(c) The distribution of macroscopic residual oil after foam flooding

Fig. 33 shows the experimental results of foam flooding in the

3D visual physical model of fractured-vuggy reservoir. Foam flooding displaced the residual oil (Macro-2 and Macro-3) in both underground rivers that could not be effectively swept by water flooding and gas flooding. There was still residual oil (Macro-3) in the underground river that was not effectively displaced by foam flooding. And the residual oil (Macro-4) submerged by the bottom water at the lower part of fractured-vuggy reservoir still could not be swept by foam flooding.

Fig. 34 shows the distribution of residual oil in the fractured-vuggy reservoirs with different displacement methods. The results show that gas flooding could effectively sweep the attic oil, but had no effect on the displacement of other types of residual oil. However, foam flooding could effectively sweep different types of residual oil after water and gas flooding. Foam could effectively sweep three kinds of microscopic residual oil (Micro-1, Micro-2 and Micro-3) and three kinds of macroscopic residual oil (Macro-1, Macro-2 and Macro-3) in fractured-vuggy reservoirs. This indicates that foam has a good application potential to improve the recovery ratio of fractured-vuggy reservoirs.

#### 5. Conclusions

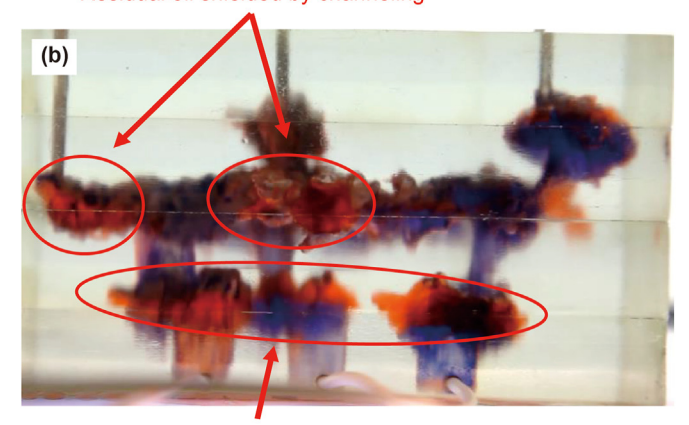
In this study, a 2D visual physical model of fractured-vuggy structure and a 3D visual physical model of fractured-vuggy

Y.-C. Wen, J.-R. Hou, X.-L. Xiao et al. Petroleum Science 20 (2023) 1620–1639

#### Residual oil shielded by channeling



#### Residual oil shielded by channeling



Residual oil disturbed by bottom water

Fig. 33. The distribution of residual oil after foam flooding in the 3D visual physical model.

Not Effectively	Micro residual oil			Macro residual oil				
Effectively sweep	Oil film (Micro-1)	Residual oil in pore and throat (Micro-2)	Residual oil in the corner (Micro-3)	Residual oil at blind end vug (Micro-4)	Attic oil (Macro-1)	Residual oil shielded by channeling (Macro-2)	Bypassed residual oil in connected fractured-vuggy structure (Macro-3)	Residual oil disturbed by bottom water (Macro-4)
Water flooding								
Gas flooding								
Foam flooding								

Fig. 34. The distribution of residual oil after water flooding, gas flooding, and foam flooding in fractured-vuggy reservoirs.

reservoir were established based on similarity criteria. The experimental study of foam flooding in these models were carried out using high stability foam. The sweep mechanisms of foam in fractures and vugs were revealed and the distribution of residual oil after foam flooding was clarified. This study gained some insights into the feasibility of foam EOR in fractured-vuggy reservoirs.

- (1) Foam can effectively improve the mobility ratio and control the fluid velocity in the horizontal direction of fractured vuggy reservoirs. It can sweep varying aperture fractures and displace residual oil in complex fracture networks.
- (2) Foam can effectively weaken the influence of gravity segregation in the longitudinal direction of fractured vuggy reservoirs. It can inhibit the injected fluid from migrating along high-angle fractures and effectively displace the residual oil in high-angle fractured-vuggy structures.
- (3) The effect of foam flooding in fractures can be improved by increasing the strength of foam and enhancing the stability of foam. The effect of foam flooding in vugs can be improved

- by reducing the density of foam and the interfacial tension between foam and oil.
- (4) Foam can effectively sweep different kinds of residual oil after water flooding and gas flooding in fractured-vuggy reservoirs. Three kinds of microscopic residual oil and three kinds of macroscopic residual oil can be displaced by foam flooding. The recovery ratio of fractured-vuggy reservoirs can be further improved by conducting foam flooding after water and gas flooding.
- (5) The EOR of foam in fractured-vuggy reservoirs is verified by foam flooding in the 3D visual physical model. The recovery ratio of foam flooding is at least 10% higher than that of gas flooding.

#### **Declaration of competing interest**

The authors declare that they have no known competing financial interests or personal relationships that could have appeared to influence the work reported in this paper.

#### **Acknowledgements**

This work was financially supported by Project of Sinopec Northwest Oilfield Company (Grant No. 202108ZB0046).

#### References

- Chen, J., Sun, S.Y., Wang, X.P., 2014. A numerical method for a model of two-phase flow in a coupled free flow and porous media system. J. Comput. Phys. 268, 1–16. https://doi.org/10.1016/j.jcp.2014.02.043.
- Chen, Z.H., Dai, Y., Lang, Z.X., 2005. Storage-percolation modes and production performance of the karst reservoirs in Tahe Oilfield. Petrol. Explor. Dev. 32 (3), 101–105. https://doi.org/10.3321/j.issn:1000-0747.2005.03.025 (in Chinese).
- Dai, C.L., Fang, J.C., Jiao, B.L., et al., 2018. Development of the research on EOR for carbonate fractured-vuggy reservoirs in China. J. China Univ. Petrol. 42 (6), 67–78. https://doi.org/10.3969/j.issn.1673-5005.2018.06.008 (in Chinese).
- Gee, B., Gracie, R., 2022. Beyond Poiseuille flow: a transient energy-conserving model for flow through fractures of varying aperture. Adv. Water Resour. 164, 104192. https://doi.org/10.1016/j.advwatres.2022.104192.
- Hou, J.R., Luo, M., Zhu, D.Y., 2018. Foam-EOR method in fractured-vuggy carbonate reservoirs: mechanism analysis and injection parameter study. J. Petrol. Sci. Eng. 164, 546–558. https://doi.org/10.1016/j.petrol.2018.01.057.
   Hou, J.R., Zheng, Z.Y., Song, Z.J., et al., 2016. Three-dimensional physical simulation
- Hou, J.R., Zheng, Z.Y., Song, Z.J., et al., 2016. Three-dimensional physical simulation and optimization of water injection of a multi-well fractured-vuggy unit. Petrol. Sci. 13 (2), 259–271. https://doi.org/10.1007/s12182-016-0079-4.
- Li, J.L., Chen, Z.H., Gao, S.S., 2009. Microcosmic experiment modeling on water-driven-oil mechanism in fractured-vuggy reservoirs. Petrol. Geol. Exper. 31 (6), 637–642. https://doi.org/10.11781/sysydz200906637 (in Chinese).
- Li, Y., Fan, Z.H., 2011. Developmental pattern and distribution rule of the fracture-cavity system of Ordovician carbonate reservoirs in the Tahe Oilfield. Acta Pet. Sin. 32 (1), 101–106. https://doi.org/10.7623/syxb201101015 (in Chinese).
- Liang, T., Hou, J.R., Qu, M., et al., 2021. Flow behaviors of nitrogen and foams in micro-visual fracture-vuggy structures. Roy. soc. Chem. 11 (45), 28169–28177. https://doi.org/10.1039/D1RA04474E.
- Liu, L.J., Huang, Z.Q., Yao, J., et al., 2020. An efficient hybrid model for 3D complex fractured vuggy reservoir simulation. SPE J. 25 (2), 907–924. https://doi.org/10.2118/199899-PA
- Lu, G., Zhang, L.H., Liu, Q., et al., 2022. Experiment analysis of remaining oil distribution and potential tapping for fractured-vuggy reservoir. J. Petrol. Sci. Eng. 208, 109544. https://doi.org/10.1016/j.petrol.2021.109544.
- Qu, M., Hou, J.R., Qi, P.P., et al., 2018. Experimental Study of fluid behaviors from water and nitrogen floods on a 3-D visual fractured-vuggy model. J. Petrol. Sci. Eng. 166, 871–879. https://doi.org/10.1016/j.petrol.2018.03.007.
- Qu, M., Hou, J.R., Wen, Y.C., et al., 2020a. Nitrogen gas channeling characteristics in fracture-vuggy carbonate reservoirs. J. Petrol. Sci. Eng. 186, 106723. https:// doi.org/10.1016/j.petrol.2019.106723.
- Qu, M., Hou, J.R., Liang, T., et al., 2020b. Synthesis of α-starch based nanogel particles and its application for long-term stabilizing foam in high-salinity, high-temperature and crude oil environment. J. Petrol. Sci. Eng. 191, 107185. https://doi.org/10.1016/j.petrol.2020.107185.
- Rong, Y.S., Huang, Y.M., Liu, X.L., et al., 2008. Single well water injection production

- in Tahe fracture-vuggy reservoir. Petrol. Drill. Techniq. 36 (4), 57–60. https://doi.org/10.3969/j.issn.1001-0890.2008.04.015 (in Chinese).
- Rong, Y.S., Li, X.H., Liu, X.L., et al., 2013. Discussion about pattern of water flooding development in multi-well fracture cavity units of carbonate fracture-cavity reservoir in Tahe oilfield. Petrol. Geol. Recov. Effic. 20 (2), 58–61+115. https://doi.org/10.3969/j.issn.1009-9603.2013.02.015 (in Chinese).
- Song, Z.J., Hou, J.R., Liu, Z.C., et al., 2016. Nitrogen Gas Flooding for Naturally Fractured Carbonate Reservoir: Visualisation Experiment and Numerical Simulation. SPE Asia Pacific Oil & Gas Conference and Exhibition. Society of Petroleum Engineers. https://doi.org/10.2118/182479-MS.
- Su, W., Hou, J.R., Zhao, T., et al., 2017. Experimental investigation on continuous N<sub>2</sub> injection to improve light oil recovery in multi-wells fractured-cavity unit. Petroleum 3 (3), 367–376. https://doi.org/10.1016/j.petlm.2017.03.002.
- Talebian, S.H., Masoudi, R., Tan, I.M., et al., 2014. Foam assisted CO<sub>2</sub>-EOR: a review of concept, challenges, and future prospects. J. Petrol. Sci. Eng. 120, 202–215. https://doi.org/10.1016/j.petrol.2014.05.013.
- Telmadarreie, A., Trivedi, J., 2017. Evaluation of foam generated with the hydrocarbon solvent for extra-heavy oil recovery from fractured porous media: porescale visualization. J. Petrol. Sci. Eng. 157, 1170—1178. https://doi.org/10.1016/j.petrol.2017.08.035.
- Wang, J., Ji, Z.M., Liu, H.Q., et al., 2019. Experiments on nitrogen assisted gravity drainage in fractured-vuggy reservoirs. Petrol. Explor. Dev. 46 (2), 355–366. https://doi.org/10.1016/S1876-3804(19)60015-7.
- Wang, J., Liu, H.Q., Xu, J., et al., 2012. Formation mechanism and distribution law of remaining oil in fracture-cavity reservoirs. Petrol. Explor. Dev. 39 (5), 585–590. https://doi.org/10.1016/S1876-3804(12)60085-8 (in Chinese).
- Wang, J., Zhao, W., Liu, H.Q., et al., 2020. Inter-well interferences and their influencing factors during water flooding in fractured-vuggy carbonate reservoirs. Petrol. Explor. Dev. 47 (5), 1062–1073. https://doi.org/10.1016/S1876-3804(20) 60117-3.
- Wang, X.W., Chen, J.J., Lv, C., et al., 2015. Experimental investigation and evaluation on influence of foam flow resistance in porous media. Environ. Earth Sci. 74 (7), 5729–5738. https://doi.org/10.1007/s12665-015-4590-5.
- Wen, Y.C., Qu, M., Hou, J.R., et al., 2019. Experimental study on nitrogen drive and foam assisted nitrogen drive in varying-aperture fractures of carbonate reservoir. J. Petrol. Sci. Eng. 180, 994–1005. https://doi.org/10.1016/j.petrol.2019.06.028.
- Xie, H.J., 2019. Formation Mechanism of Remaining Oil for Fractured-Vuggy Carbonate Reservoirs Considering Filling Medium. Ph.D. Dissertation. (in Chinese). China University of Petroleum, East China.
- Yang, H.B., Iqbal, M.W., Lashari, Z.A., et al., 2019. Experimental research on amphiphilic polymer/organic chromium gel for high salinity reservoirs. Colloids Surf. A Physicochem. Eng. Asp. 582, 123900. https://doi.org/10.1016/ j.colsurfa.2019.123900.
- Yang, J.B., Hou, J.R., 2020. Experimental study on gas channeling characteristics of nitrogen and foam flooding in 2-D visualized fractured-vuggy model. J. Petrol. Sci. Eng. 192, 107334. https://doi.org/10.1016/j.petrol.2020.107334.
- Yuan, D.Y., Hou, J.R., Song, Z.J., et al., 2015. Residual oil distribution characteristic of fractured-cavity carbonate reservoir after water flooding and enhanced oil recovery by N<sub>2</sub> flooding of fractured-cavity carbonate reservoir. J. Petrol. Sci. Eng. 129, 15–22. https://doi.org/10.1016/j.petrol.2015.03.016.